EFFECT OF THE WATER DISINFECTANT CHLORINE DIOXIDE ON THE INTEGRITY OF A REVERSE OSMOSIS MEMBRANE

BY

KENTARO MIZUTA

THESIS

Submitted in partial fulfillment of the requirements
for the degree of Master of Science in Environmental Engineering in Civil Engineering
in the Graduate College of the
University of Illinois at Urbana-Champaign, 2014

Urbana, Illinois

Adviser:

Professor Benito J. Mariñas

ABSTRACT

Chlorine dioxide has been used as a water disinfectant in water reclamation plants prior to the emergence of RO membrane process. However, the effects of chlorine dioxide on the integrity of RO membranes have yet to be fully understood. In this study, the influence of chlorine dioxide on RO membranes was investigated by observing chlorine dioxide reactions in the presence of iodide and bromide, structural changes of the RO membrane active layer polyamide and evolution in RO membrane assesses a solute passage (Rhodamine WT) and water flux. Batch experiments were performed to assess the reaction of chlorine dioxide, bromide and iodide in a potassium phosphate (10mM) buffered solution (pH=7.5). Iodide was found to react with chlorine dioxide over time while bromide did not under condition relevant to water treatment. On the other hand, chlorine dioxide oxidized bromide when the bromide concentration exceeded that of chlorine dioxide. Investigation of the influence of these compounds on the RO membrane polyamide using Rutherford back-scattering spectrometry (RBS) revealed that polyamide was underwent bromination but was more resistant to chlorination and iodination. These results suggest that chlorine dioxide oxidizes bromide although the reaction is slow, and it leads to polyamide bromination. Furthermore, RO membranes exposed to chlorine dioxide and bromide had significantly decreased the solutes rejection and water flux, while exposure to chlorine dioxide alone had no measureable influence. Therefore, we found that chlorine dioxide oxidation of bromide specifically leads to polyamide bromination and RO membrane deterioration.

ACKNOWLEDGEMENTS

First of all, I would like to express my deepest gratitude to the Japan Sewage Works Agency for financial support throughout the course of this study based on the Japanese Engineers Exchange Program under the Trilateral Training Agreement between United States Environmental Protection Agency, Department of Civil Engineering, University of Illinois at Urbana-Champaign (UIUC), and Japan Sewage Works Agency (JSWA).

I also would like to show my greatest appreciation to my academic advisor, Professor Benito J. Mariñas, for his dedicated support, valuable advice and arrangement of this program.

I also thank Lauren Valentino for providing her expertise and knowledge about RBS analysis and supporting me throughout this research project. Advice and comments given by her were essential for accomplishing this study. I am thankful to Dr. Ana Martinez for training in RBS operation and permeation experiments during her time as a PhD student at the University of Illinois. I am also thankful Dr. Susana Kimura for supporting ClO_2 generation, UV-VIS analysis and sharing her knowledge about kinetics analysis. I also thank the rest of the other students in the Mariñas research group and in my office. I would like to offer my special thanks to my colleague of Japan Sewage Works Agency for their sincere encouragement and technical support.

Special thanks to Doug Jeffers at the Center of Microanalysis of Materials, University of Illinois at Urbana-Champaign for assistance operating the RBS.

I want to thank my parents, Yoji and Saeko for their continuing and tremendous support. I also thank my family-in-law for their huge help and understanding.

Finally, my heartfelt appreciation goes to my wife, Eri, my daughters, Mana and Hina. Without their understanding of my study and moral support, this thesis would not have been possible.

TABLE OF CONTENTS

CHAPTER 1

INTRODUCTION

Producing safe drinking water is essential because water scarcity is a universal issue, especially in developing countries. Membrane separation systems allow removal of various chemicals such as salts, metals and organic compounds in the feed water, whereby improving water quality. Reverse osmosis (RO) membranes, which have a high selectivity and durability, are implemented in desalinization plants and discharged wastewater purification plants to produce safe water.

There are several types of RO membranes, such as thin film composite, asymmetric cellulose triacetate, hollow fiber membranes and ceramic membranes. Thin film composite (TFC) RO membranes consist of an active layer (around 200 nm), support layer (up to 50μm) and polyester fabric (Figure 1). Membranes are folded with permeate carrier inside, and the resulting sheets are rolled around a permeation collection tube. The active layer is made of fully aromatic polyamide (PA, $C_{36}H_{24}N_6O_6$) which function is to remove salts and organic compounds. The support layer is made of polysulfone (PS, $C_{27}H_{26}O_6S$). The active layer is formed by interfacial polymerization on the surface of the support layer. The polyester fabric supports these two layers with the necessary mechanical properties (Coronell et al., 2008, Petersen 1993).

TFC RO membranes are commonly used because of their higher permeability and ability to select against a variety of contaminants. However, they cannot be used semi-permanently due to vulnerability to fouling caused by accumulation of undesirable materials on the membrane surface. This clogs the membrane pores and reduces permeate flux. Such fouling includes formation of cake layer, biofouling, organic fouling and inorganic fouling (Meng et al., 2009).

Biofouling or cake layer formation is caused by the deposition, growth and metabolism of bacteria cells or flocs on the membranes (Pang et al., 2005). In general, it is prevented by feed water disinfection. Although oxidizing agents are usually used as disinfectants to the feed water of RO membranes, some disinfection by-products (DBPs) are not only harmful to human health, but they can also damage the RO membrane. For example, Antony et al. (2010) indicated that oxidation of polyamide on the RO membrane with free chlorine results in the degradation of salt rejection and membrane permeability in some cases. Furthermore, Silva et al. (2006) concluded that the degradation of polyamide with monochloramine would have a similar effect as free chlorine, albeit to a lesser extent.

Several mechanisms that result in morphological and chemical changes have been studied (Glater et al., 1983, Singh 1994 and Kang et al., 2007). A study by Kang et al (2007) characterized a two-stage mechanism for chlorine-mediated polyamide degradation in which hypochlorite chlorinates the polyamide N and the unstable N-chlorinated amides undergo an irreversible Orton Rearrangement (Kang et al., 2007) that results in polyamide deterioration and decrease in RO membrane integrity (Figure 2). Gabelich (2005) indicated that the formation of Cl(Ⅰ) is the primary driver in polyamide membrane chlorination reactions. Due to the similarity in properties and behavior, it is reasonable to assume that bromine or iodine in the +1 oxidation state also drive bromination and iodination reactions of the polyamide membrane. In fact, polyamide type membranes are sensitive to chlorine significantly (Glater, 1981).

CHLORINE DIOXIDE

Chlorine dioxide is also an oxidizing agent used as a water disinfectant prior to RO membrane filtration units in some drinking water treatment processes (Junli et al., 1997). Typically, chlorine dioxide is applied to reach 0.1 – 5.0 mg/L in drinking water treatment (Tzanavaras et al.,

2007). Although the handling is difficult due to the high Henry's constant and vulnerability to UV-mediated degradation, chlorine dioxide has a higher oxidation potential than chlorine but it generates a less number of DBPs (Agus et al., 2009, Aieta, 1986, Rav-Acha, 1985, Richardson et al., 2000). Therefore, chlorine dioxide can be used as a water disinfectant with shorter contact time and lower DBPs production than chlorine. Heijne (1973) indicated that the ClO_2 decomposition rate is quite slow in neutral aqueous solutions. Bray (1906) proposed chlorine dioxide decomposition in basic condition as follows;

$$2ClO_2 + 2OH^- \rightarrow ClO_2^- + ClO_3^- + H_2O \quad (1)$$

$$-\frac{\mathrm{d}[ClO_2]}{\mathrm{dt}} = k[OH^-][ClO_2]^2 \quad (2)$$

where, the rate constant *k* is 15.3 M^{-2} S^{-1}. In addition, Odeh et al. (2002) proposed three concurrent chlorine dioxide decay pathways showing that, at low ClO_2 concentrations, ClO_2^- yield is greater than that of ClO_3^-.

Iodide and bromide reactions with chlorine dioxide has been studied by many researchers (Odeh, et al., 2002, Fábián, 1997, Fukutomi, 1967, Hoigne and Bader, 1994, Lengyel et al., 1996). Fábián (1997) and Fukutomi (1967) indicated that, under near neutral pH conditions, the iodide-mediate reaction proceeds as follows;

$$2ClO_2 + 2I^- \rightarrow 2ClO_2^- + I_2 \quad (3)$$

where, the rate constant k of intermediate $[ClO_2 \cdot I^-]$ is $(1.87\pm0.02)\times10^3$ M^{-1} s^{-1} (Fábián, 1997) and 2.95×10^3 M^{-1} s^{-1} (Fukutomi, 1967) at 25℃, respectively. In addition, Hoigne and Bader (1994) observed that iodide is easily oxidized by chlorine dioxide (the rate constant $k = 1.4\times10^3$ M^{-1} s^{-1}) although the product has not been clearly identified. On the other hand, there are some studies that hypoiodite is produced after the iodine production (Eigen, 1961 and Bichsel, 2000).Therefore, the iodide reaction with chlorine dioxide remains unclear.

As for bromide, most researchers argued that chlorine dioxide does not oxidize bromide (Agus, 2009, Belluati et al., 2007, and Hoigne, 1994). However, Agus (2009) suggested that further investigation should be conducted in order to figure out the bromide reaction with chlorine dioxide.

In terms of the polyamide degradation with chlorine dioxide, Glater (1983) concluded that polyamide membranes are not damaged by chlorine dioxide at near neutral pH since halogen uptake was not observed. Furthermore, using X-ray photoelectron spectroscopy (XPS), Sandín et al (2013) compared the extent of polyamide membranes chlorination when exposed to hypochlorite and chlorine dioxide. As a result, they observed that exposure to chlorine dioxide led to one third chlorination less than hypochlorite, demonstrating that chlorine dioxide leads to less halogenation than chlorine. However, as XPS can analyze down to 5 nm depth below the membrane surface, Bartels (1989) indicated that the elemental compostion of active layer could vary with depth. Therefore, these data only represent the surface of membrane active layer.

Kwon et al. (2011) and Sandín et al. (2013) indicated that the membrane exposure to chlorine dioxide and bromide preferrentially led to polyamide bromination rather than chlorination. This evidences that hypobromite is produced in the presence of chlorine dioxide and bromide. However, it is contradictory to the above that chlorine dioxide does not oxidize bromide (Agus, 2009, Belluati et al., 2007, and Hoigne, 1994).

RUTHERFORD BACKSCATTERING SPECTROMETRY

Rutherford Backscattering Spectrometry (RBS) is an analytical technique that can be used to assay the elemental composition of membrane layers. While XPS can only measure down to 5 nm in depth from the membrane surface, RBS can analyze approximately 2 μm; thus, RBS can measure the chemical composition of both the active layer and support layer of RO membranes. In fact, there are several studies using RBS for the analysis of membrane layers. Mi et al. (2007)

applied RBS to characterize the partitioning of arsenic (III) from aqueous phase into the active layer of NF/RO membranes. They concluded that RBS analysis provides accurate information on the elemental composition of the active layer and support layer of RO membranes. Coronell et al. (2008) used RBS to quantify the ion probes in the RO membrane's active layer. Saenz de Jubera et al. (2012) quantified the concentration of carboxylate groups associated with polyamide cross-linking in the NF membranes' active layer. Therefore, RBS is a useful instrument to analyze the elemental composition of RO membranes.

OBJECTIVES

The main objective of this study is to clarify how chlorine dioxide disinfection affects RO membrane integrity. First, the chlorine dioxide reactions with iodide and bromide were investigated with UV-VIS spectrophotometer (UV). Second, the changes in elemental compositions of RO membranes that were exposed to chlorine dioxide, iodide and bromide solutions, were analyzed by RBS. Third, solute rejection and water flux were evaluated through testing the permeability of disinfectant-exposed RO membranes. Finally, the structural effects of RO membranes were evaluated based on the solute transport model used by Saenz de Jubera et al. (2012).

CHAPTER 2

MATERIALS AND METHODS

CHLORINE DIOXIDE

Chlorine dioxide was produced by the method reported by Vicuña et al. (2008). In this method, chlorine dioxide can be produced from chlorine gas and solid sodium chlorite as follows;

$$2\mathrm{NaClO_2} + Cl_2 \rightarrow 2\mathrm{ClO_2} + 2NaCl \quad (5)$$

The gas/solid reaction took place in a bench scale generator system (CDG Technology, Bethlehem, PA). In this system, pure chlorine gas (40,000 ppmv) is injected into a cartridge and containing sodium chlorite where it reacts. All tubes are made of Teflon© to prevent side reactions. A leak test was conducted every time by nitrogen gas before using the system. Then, chlorine gas was injected with an inlet pressure of approximately 10 psig. Since the chlorine dioxide gas at a concentration of approximately 77,000 ppmv was generated as gaseous matter, the gas was bubbled through a diffuser into a 120 mL amber bottle with Nanopure water. Approximately, 25 mM ClO_2 solution was produced after 2-3 minutes bubbling. After finishing the chlorine dioxide gas production, the system was purged by nitrogen gas for 15 minutes. Chlorine dioxide solution was prepared fresh and stored in a dark room at 4℃ before each experiment as it is sensitive to temperature and light.

CHLORINE DIOXIDE REACTION WITH IODIDE AND BROMIDE

The reactions of chlorine dioxide with iodide and bromide were investigated using 120 ml amber bottles as reactors. The following conditions were tested;

(1) 20 mg/L (0.30 mM) ClO_2

(2) 20 mg/L (0.30 mM) ClO_2 and 0.50 mg/L (3.9×10^{-3} mM) I

(3) 20 mg/L (0.30 mM) ClO_2 and 20 mg/L (0.25 mM) Br

(4) 20 mg/L (0.30 mM) ClO_2, 0.50 mg/L (3.9×10^{-3} mM) I and 20 mg/L (0.25 mM) Br

(5) 2 mg/L (0.030 mM) ClO_2

(6) 2 mg/L (0.030 mM) ClO_2 and 0.050 mg/L (3.9×10^{-4} mM) I

(7) 2 mg/L (0.030 mM) ClO_2 and 2.0 mg/L (0.025 mM) Br

(8) 2 mg/L (0.030 mM) ClO_2, 0.050 mg/L (3.9×10^{-4} mM) I and 2.0 mg/L (0.025 mM) Br

Iodide and bromide solutions were prepared with potassium iodide (KI) and potassium bromide (KBr), both buffered at pH 7.5 with potassium phosphate buffer solution. Batch experiment solutions (1) to (8) were sampled every 24 hours for 10 days. For each sample, chlorine dioxide concentration was measured with a UV-Visible spectrophotometer (UV-2610 Shimadzu, JAPAN) using a 1 cm quartz cell. The concentration was calculated using the following absorbance-concentration conversion equation:

$$C = \frac{A \cdot MW \cdot 1000}{\varepsilon \cdot l} \times 10^{-3} \quad (6)$$

Where A is the absorbance, MW is the molecular weight of chlorine dioxide (67.45 g/mole). And *l* is the light path length (1 cm). According to Furman (1998), the molar absorptivity (ε) of chlorine dioxide is 1230 L M^{-1} cm^{-1} at 359 nm. For samples with absorbance exceeding 1.0, samples were diluted to prevent deviation from Beer's law.

In addition, chlorine dioxide reaction with different bromide concentrations were observed by setting up batch experiments with constant chlorine dioxide concentrations (20 mg/L or 0.296 mM) and varied bromide concentrations (0 mg/L, 2000 mg/L (0.025 M), 4000 mg/L (0.050 M), 6000 mg/L (0.075 M)).

MEMBRANE LAYERS ANALYSIS WITH RBS

RO membrane coupons were soaked in the above solutions (1) to (8) plus in an additional control of 10mM phosphate buffer solution. In this study, SW30HR (DOW FilmTec Co., USA)

thin-film composite RO membrane coupons were used. Membrane coupons were rinsed in Nanopure water (Thermo Scientific Barnstead Dubuque, IA) for at least 24 hours prior to use. To observe the extent of membrane damage over time, batch experiments were conducted. The membrane coupons were sampled at 1, 2, 5, 12, 24, 48, 96, 144 and 240 hours for each treatment. Sampled membrane coupons were rinsed in 1:1000 dilutions of their respective solutions for 30 minutes.

After the batch experiments, membrane coupons were dried for at least 24 hours and analyzed by RBS. Sampled membrane coupons were attached onto the sample stage by double-sided thermal conductive tape (T410 material, Marian, Chicago, IL).

In order to measure the elemental composition, a Van de Graaf accelerator (High Voltage Engineering Corp., Burlington, MA) was used. This accelerator can direct a 3 mm diameter 2 MeV helium beam against a membrane layer, and the measured RBS spectra were analyzed using SIMNRA (Max-Planck-Institut fur Plasmaphysik, Garching, Germany). To prevent membrane damage by exceeding the helium ion fluence threshold, the stage was continuously moved (Mi et al., 2007). The measurements were completed when approximately 1000 counts of carbon were collected for each sample. This allowed determination of the active and support layer chemical composition at an atomic density of 10^{15} atoms/cm^2. The spectra were normalized to the sulfur plateau. Based on the composition data, molar concentrations of bromine and iodine in the active layer were calculated with the following equations (Coronell et al., 2011)

$$[\mathrm{Br}] = \varepsilon'_{Br} \times \frac{\rho_{PA}}{\sum_{C,O,N,Cl,H}(\varepsilon'_i \times M_i)} \quad (7)$$

$$[\mathrm{I}] = \varepsilon'_{I} \times \frac{\rho_{PA}}{\sum_{C,O,N,Cl,H}(\varepsilon'_i \times M_i)} \quad (8)$$

Where ε'_I, M_i and $\rho_{PA} = 1.24\ \mathrm{g}/cm^3$ are the elemental fraction of element i, molar mass of element i, and density of polyamide, respectively.

PERMEATION TEST

For fabrication and performance characterization of exposed membranes as mentioned in above, a dead-end membrane filtration apparatus (model 8400, Millipore Co., Bedford, MA) was used (Suzuki et al., 2007, Saenz de Jubera et al., 2012, Saenz de Jubera et al., 2013). Permeate flow rates were monitored gravimetrically with an analytical balance (BP211S, Sartorius Co., Edgewood, NY) connected to a computer. All membrane fabrication and performance characterization experiments were performed at room temperature (22−25 °C) under magnetic stirring.

Permeation experiments were performed with single-solute aqueous solutions containing 2.5 mg/L Rhodamine WT (R-WT). NaH_2PO_4 and Na_2HPO_4 were used to adjust the pH to 7.5 for the R-WT solutions. R-WT (35% (w/v) aqueous solution, Turner Designs, Sunnyvale, CA) with a molar mass of 487 g/mol was used as a representative of organic contaminants (Saenz de Jubera et al., 2012). The performance of each membrane was measured at varying hydraulic pressures within the range of 0.10 – 0.41 MPa. Both feed solutions and permeate solutions at each hydraulic pressures were taken after the flux was stable.

R-WT was measured by fluorescence (excitation/emission wavelength of 556/580 nm) using a spectrofluorometer (RF-5301 PC, Shimadzu, Scientific Instruments, Inc.).

SOLUTE TRANSPORT MODEL

The solute passage model, used by Saenz de Jubera et al. (2012), was applied to the results obtained from permeation experiments with R-WT. This model was developed based on a modified version of the diffusion model (Wijmans and Baker, 1995) that accounts for the existence of imperfections in the active layer through which advective transport occurs (Urama, 1997).

According to Urama (1997), the water and solute fluxes through the membrane at steady state can be expressed as follows;

$$J_v = A_D(\Delta p - \Delta\pi)/(1-\alpha) \quad (9)$$

$$J_s = J_V C_P = \mathrm{B}(C_w - C_P) + \alpha J_V C_w \quad (10)$$

$$\Delta\mathrm{p} = p_f - p_p \quad (11)$$

$$\Delta\pi = \pi_f - \pi_p \quad (12)$$

Where J_V ($m^3/m^2/d$) and J_S ($mol/m^2/d$) are the product water and solute fluxes, A_D ($m^3/m^2/d/Mpa$) and B (m/d) are the product water and solute permeation coefficients, α is the fraction of the total product water flux corresponding to advection through membrane imperfections, p_f and π_f are the hydraulic pressure and osmotic pressure of feed water, p_p and π_p are the hydraulic pressure and osmotic pressure of product water, Δp and Δπ are the differences in hydraulic and osmotic pressure across the membrane active layer, respectively, C_P, C_w and C_P are the solute concentration of bulk feed solution, feed solution next to the membrane wall, and permeate, respectively.

The feed water concentration side adjacent to the membrane surface can be represented with the following concentration-polarization expression (Mathiason and Sivik, 1980);

$$\frac{C_w - C_p}{C_f - C_p} = exp\left(\frac{J_v}{k}\right) \quad (13)$$

where *k* (m/d) is the solute mass transfer coefficient in the concentration-polarization film. In this study, $k_{R\text{-}WT}$ = 1 m/d reported by Saenz de Jubera et al. (2012) was used for fitting the R-WT data.

Overall, solute permeability (SP = C_p/C_f) could be expressed as follows (Saenz de Jubera et al., 2012);

$$\mathrm{SP} = 1 - \mathrm{SR} = 1 - \frac{1}{1+\left[\frac{B}{(1-\alpha)J_v}+\frac{\alpha}{1-\alpha}\right]exp\left(\frac{J_v}{k}\right)} \quad (15)$$

where, SR represents solute rejection (1- C_p/C_f).

CHAPTER 3

RESULTS AND DISCUSSION

CHLORINE DIOXIDE REACTION

ClO_2 reaction with bromide and iodide were observed by UV-VIS spectra analysis. Figure 3 shows the temporal ClO_2 concentration profile in absence, presence, and simultaneous presence of bromide and iodide. Experimental conditions correspond to absence of Br and I, 20 mg/L Br, 0.5 mg/L I, 20mg/L Br and 0.5 mg/L I solutions containing initially 20mg/L ClO_2 with the pH adjusted to 7.5 with 10 mM phosphate buffer solution. Additional results and raw data were shown in Figure A1 and Table A1 to Table A8 of the Appendix.

As shown in Figure 3, ClO_2 concentration decreased over time during the experiment with regard to the iodide solution. According to the eq. (3) and some studies (Fábián, 1997 and Fukutomi, 1967), I_2 is produced as a result of ClO_2 reaction with iodide. Since the ClO_2 decrease ratio is determined by the rate constant, ClO_2 concentration and I^- concentration, the ClO_2 decrease ratio decreases with the consumption of ClO_2 and I^-. The temporal change in ClO_2 concentrations in the presence of iodide can be estimated using eq. (1), (2) and (3). However, models based on eq. (1) and (2) did not fit the measured ClO_2 self-decomposition for treatments with 20 mg/L ClO_2 and 2 mg/L ClO_2, as shown in Figure 4. This discrepancy may be attributed to ClO_2 volatilization due to its relatively high volatility (K_H = 0.85 to 1.0 M/atm) (Sander, 1999). Although eq. (2) and (3) were not used due to the sampling issues, the results revealed that iodine was formed as a result of the ClO_2 reaction with iodide as Fábián (1997) and Fukutomi (1967) previously observed.

On the other hand, ClO_2 did not appear to decay in the 20 mg/L Br solution. This result was consistent with previous studies suggesting that chlorine dioxide does not oxidize bromide (Agus, 2009, Belluati et al., 2007, and Hoigne, 1994). However, the ClO_2 concentration in the 20

mg/L Br and 0.5 mg/L I solution also did not decrease as much as that in the 0.5 mg/L I solution. This result indicates that bromide works to retard the reaction of ClO_2 and iodide, or bromide is oxidized by chlorine dioxide.

In order to assess of ClO_2 under a slower reaction with bromide, higher bromide concentrations (200 mg/L Br, 2000 mg/L Br, 4000 mg/L Br and 6000 mg/L Br) were applied in comparison with ClO_2 concentration (20 mg/L). As shown in Figure 5, ClO_2 concentration decreased over time, and the rate of decrease was more pronounced at higher bromide concentration. Furthermore, a specific absorbance peak was appeared around 266 nm wavelength as shown in Figures A3, A4 and A5. According to Gazda (1994) and Sasulard (1981), the 266 nm wavelength is tribromide (Br_3^-) of which molar absorptivity (ε) is 35000 L M^{-1} cm^{-1}.Therefore Br_3^- concentration can be estimated by eq. (6). Figure 6 indicates the Br_3^- concentration profile over time in case of 200 mg/L Br, 2000 mg/L Br, 4000 mg/L Br and 6000 mg/L Br disinfected with 20 mg/L ClO_2. As shown in Figures 5 and 6, Br_3^- concentration increased with the decrease of ClO_2 concentration. According to Gazda (1994), Br_3^- is formed by following equation;

$$Br_2 + Br^- \overset{k_{Br_3}}{\longleftrightarrow} Br_3^- \tag{16}$$

$$Br_2 = \frac{[Br_3^-]}{k_{Br_3} \cdot [Br^-]} \tag{17}$$

Where, k_{Br_3} is 16.6 M^{-1}. Assuming that Br_2 is formed by the same pathway of the iodide reaction with ClO_2, Br_2 forming reaction can be expressed as follows;

$$2ClO_2 + 2Br^- \rightarrow 2ClO_2^- + Br_2 \tag{18}$$

On the other hand, Fickert (1999) indicated that HOBr is formed in the presence of Br_2 as shown in the following equation.

$$Br_2 + (H_2O) \xrightarrow{k_{HOBr}} \mathrm{HOBr} + Br^- + H^+ \tag{19}$$

$$\mathrm{HOBr} + Br^- + H^+ \xrightarrow{k_{Br_2}} Br_2 + H_2O \quad (20)$$

Where, $k_{HOBr} = 110s^{-1}$, $k_{Br_2} = 1.6 \times 10^{10} M^{-2} S^{-1}$. Overall, eq. (19) and eq. (20) can be expressed as follows;

$$\mathrm{Br}_2 + H_2O \xleftrightarrow{k_{eqHOBr}} HOBr + Br^- + H^+ \quad (21)$$

$$k_{eqHOBr} = \frac{k_{HOBr}}{k_{Br_2}} = 6.9 \times 10^{-9} \quad (22)$$

$$[\mathrm{HOBr}] = \frac{[Br_2]}{[Br^-][H^+]} k_{eqHOBr} \quad (23)$$

Substituting eq. (17) into eq. (23), HOBr is calculated as follows;

$$[\mathrm{HOBr}] = \frac{[Br_3^-]}{[Br^-][H^+]} \cdot \frac{k_{eqHOBr}}{k_{Br_3^-}} \quad (24)$$

Table 1 shows the bromide and bromine compounds concentration at equilibrium. As shown in Table 1, the HOBr concentration increased with the increase of bromide, presumably derived from ClO_2 reaction with bromide. Thus, HOBr could be produced by the reaction between ClO_2 and bromide. However, the low HOBr concentration and molar absorptivity (100 L M^{-1} cm^{-1}) limits spectrophotometric detection (Gazda (1994). This results clearly demonstrates that ClO_2 oxidize bromide and bromine compounds were formed.

MEMBRANE LAYERS ANALYSIS

Results for one of the RBS analysis of membrane exposure over time to control (10mM phosphate buffer solution) and 20 mg/l ClO_2, 20 mg/L Br and 0.5 mg/L I with 10 mM phosphate buffer solution were shown in Figure 7, 8 and Table 2 to 7, respectively. Each element peak was determined by SIMRA for RBS spectra analysis. The other RBS analysis results were shown in Figures B1 to B5 and Table B1 to B15 of the Appendix. Although neither bromine nor chlorine peaks were observed in control membranes (Figure 7), such peaks were observed in the exposed

membranes at 1.65 MeV and 1.29 MeV respectively (Figure 8). This result clearly demonstrates that the polyamide active layer on the membranes were halogenated (chlorinated, brominated) in the presence of chlorine dioxide and bromide. On the other hand, iodine peak at around 1.70 MeV was hardly observed. In addition, a small height of potassium peak at around 1.32 MeV was also observed in the exposed membranes (Figure 8). Since bromine, chlorine and potassium peaks were not observed in bromide and iodide solution without chlorine dioxide (Figure B1 and Table B1 on the Appendix), halogenation and potassium association most likely resulted from reactions of the polyamide with chlorine dioxide.

Figures 9 to 12 show chlorine, potassium, iodine and bromine concentration in the polyamide membrane active layer over time.

Although chlorine uptake was observed in all cases as shown in Figure 9, it increased rapidly reaching a plateau. The mean chlorine content in polyamide was approximately 1.8% by polyamide weight after exposure for 49 hours (Table B1 to B4 of the Appendix). Glater (1983) measured 0.3% polymer chlorine content after exposure for 48 hours with 30 mg/L ClO_2 at pH 8.6. The result was reasonably consistent with the previous research. Glater (1983) also measured 17.7% polymer chlorine content after exposure for 40 hours with 30 mg/L Cl_2 due to the PA halogenation by HOCl. Therefore, PA chlorination by ClO_2 is less pronounced than that of HOCl.

Potassium concentration increased overtime as shown in Figure 10. Alayemieka (2012) indicated that the carboxylic group in PA deprotonated ($COOH \rightarrow COO^-$) at pH above 3.5. Therefore, potassium derived from the monoionic halogen solution may associate with the negatively charged caboxylate groups.

Iodine in the PA was observed at relatively low levels (up to 0.35 % of polyamide iodination by molarity). Although I^- is oxidized to I_2 by ClO_2 as shown in eq (3), it has not been clarified yet

whether HOI is produced from I_2 or not in the presence of ClO_2. Since low iodide concentrations were used compared to bromide, iodination may be observed if a higher iodide concentration was used. In agreement, higher iodide molar concentrations for ClO_2 molar concentration indeed increased the iodine concentration in PA over time in experiments with 2 mg/l ClO_2 (0.030 mM), 0.05 mg/L I (3.9×10^{-4} mM) solution and 2 mg/l ClO_2 (0.030 mM), 0.05 mg/L I (3.9×10^{-4} mM), 2.0 mg/L Br (0.025 mM) solution. Therefore, futher studies are required to investigate the effect of ClO_2 and iodide reaction on PA.

On the other hand, the bromine concentration increased over time, reaching up to 34-41% of polyamide bromination by molarity (Figure 12). This increase of bromine concentration supports the occurrence of bromination (Sandín et al., 2013). Thus, this result clearly demonstrates that chlorine dioxide oxidize bromine and produce hypobromite. In addtion, assuming that the oxidized bromine concentration is equal to the bromination concentration of the polyamide, the bromine oxidation rate can be estimated with an equation based on the increase of bromine concentration in the polyamide.

$$\frac{\mathrm{d}[Br^-]}{\mathrm{dt}} = \frac{\Delta C_p \times A_p \times \delta_p \times 10^{-7} \times 10^{-3}}{\Delta t \times 3600 \times V} \tag{25}$$

$$\delta_p = \frac{(\sum_i M_i \varepsilon_i)\theta}{L_A \rho_p} \times 10^7 \tag{26}$$

where, $\frac{\mathrm{d}[Br^-]}{\mathrm{dt}}$ is the oxidized bromine rate (nM/sec), ΔC_p is bromine concentration at polyamide layer (mole/L PA), A_p is the total surface of exposed membrane coupons (cm^2), δ_p is the thickness of polyamide layer (nm) based on RBS analysis (Mi et al., 2006), Δt is the exposure time between a sampling to the next sampling of membrane coupons, V is the solution volume for membranes exposure (0.1 L), L_A is Avogadro's number (6.022×10^{23} atoms/mol), M_i is the atomic weight of element *i* in the membrane active layer obtained from RBS simulation expressed as elemental

fraction, ρ_p is the density of the membrane active layer (1.24 g/cm^3), and θ represents the projected atomic density of the membrane active layer (atoms/cm^2) obtained from the RBS simulation. The results are shown in Figure 13. Although there was a small difference in particular at the beginning of the experiment, the mean δ_p was 210 nm and the mean oxidized bromine rate was 3.0×10^{-2} (nM/sec) as shown in Figure 13.

PERMEATION EXPERIMENTS

Permeation experiments with Rhodamine WT were performed with RO membranes left in nanopure water for at 24 hours, exposed to 10 mM phosphate buffer solution at pH 7.5 for 10 days, and exposed to 20 mg/L ClO_2 with 0.5 mg/L I, 20 mg/L Br, 0.5 mg/L I and 20 mg/L Br, in a 10 mM phosphate buffer solution at pH 7.5 for 10 days. The water permeability (Figure 14a) and the solute passage (C_p/C_f) (Figure 14b) were plotted to assess the effect of hydraulic pressure on water permeability and the corresponding water flux J_v on solute passage. Permeation parameters for each experimental case were obtained by fitting the data with eq. (9) for water permeability and eq. (15) for solute passage.

The water flux and solute permeability increased when membranes were exposed to bromide, iodide, and both halogens along with ClO_2 disinfection in a phosphate buffer solution. The result indicates that bromination or iodination of polyamides due to the ClO_2 disinfection reduced Rhodamine WT rejection. Since different bromide and iodide concentration were used in this experiments, the effects of halogenation by each halogen on Rhodamine WT rejection cannot be compared accurately. However, comparing the membrane exposed to bromide solution disinfected by ClO_2 with the membrane exposed to mixing solution of bromide and iodide disinfected by ClO_2, the water flux and the solute permeability of the membrane exposed to bromide solution was higher than those of the membrane exposed to mixing solution of bromide

and iodide. Therefore, bromination may lead to greater damage to polyamide integrity than iodination.

On the other hand, ClO_2 improved the water permeability without affecting the Rhodamine WT rejection, comparing the membrane exposed to ClO_2 solution with the membrane exposed to phosphate buffer solution. The result is clearly consistent with the RBS result that PA was not chlorinated by chlorine dioxide. However, the result differed from Glater (1981), who argued that chlorine dioxide imposes severe damage on polyamide membranes. The reason is that Glater (1981) compared the results with untreated membranes in spite that phosphate and borate buffer were used for pH adjustment in his experiments. In fact, the water permeability and Rhodamine WT permeation of the membrane exposed to ClO_2 solution were higher than those of the unexposed membrane. Therefore, the increases of water permeability and Rhodamine WT passage may be attributed to the phosphate buffer solution, although the mechanism remains unclear. In terms of the water permeability improvement, the result was consistent with a previous study showing that water permeability was improved without any significant solute leakage (Alayemieka, 2012).

CHAPTER 4

CONCLUSIONS AND RECOMMENDATIONS

This research focused on the effect of chlorine dioxide, a disinfectant for controlling biofouling, on the integrity of a reverse osmosis membranes (pH 7.5). Although there were a number of studies addressing the effects of free chlorine on membrane integrity, this is the first study to clarify the effect of secondary oxidizing agents produced from the reactions between chlorine dioxide and bromide and iodide on the polyamide active layer of the RO membrane. The reactions between chlorine dioxide and bromide and iodide were observed by batch experiments and UV-VIS analysis. The structural and morphological effects were observed by conducting batch exposure experiments followed by RBS analysis. Finally, the effects on membrane performance were evaluated by conducting batch exposure experiments followed by permeation experiments with a dead-end membrane filtration apparatus.

Results from batch experiments and UV-VIS analysis, indicated that chlorine dioxide reacts with both bromide and iodide although the bromide reaction rate is much slower than that of the iodide reaction. In fact, small amounts of Br_3^- were observed when bromide concentration increased. The result demonstrates that HOBr could be produced from the reactions between ClO_2 and bromide although HOBr could not be spectrophotometrically detected due to its low concentration and molar absorptivity. On the other hand, as ClO_2 self-decomposition could not be fitted with the kinetics model due to ClO_2 volatilization during sampling, small doses of n-pentane were added to limit evaporation (Furman 1998). In addition, the kinetics of Br_3^- production indicated that there are multiple steps in the mechanism. Therefore, further research is required to clarify the mechanism.

RBS analysis of the batch exposure experiments revealed that there were several kinds of effects on the polyamide active layer. First, PA was significantly brominated by bromine compounds but it was not chlorinated by chlorine dioxide. This result is not only consistent with the observation that HOBr may be produced by ClO_2-mediated bromide oxidation, but also with previous observations that HOCl is not produced by the ClO_2 decomposition (Bray, 1906 and Odeh et al., 2002). With regard to iodide, iodination was not observed because HOI could not be produced from I_2 although I^- is oxidized to I_2 by ClO_2. However, since lower iodide concentrations were used in comparison with bromide concentrations in this study, additional experiments should be conducted at higher iodide concentration. In addition, it was revealed that potassium bonding with caboxylate was enhanced by ClO_2.

Permeation test indicated that bromination or iodination of polyamides due to the ClO_2 disinfection has a significant effect on RO membrane integrity in terms of the water flux and the solute rejection. Bromination resulted in larger polyamide damage than iodination. On the other hand, ClO_2 improved the water permeability without affecting solute rejections, comparing the membrane exposed to ClO_2 solution to unexposed membrane. The result is consistent with the RBS results that showed that PA was not chlorinated by chlorine dioxide. On the other hand, the effect of phosphate buffer solution should be clarified since increases of water permeability and solute passage were observed when exposed to phosphate buffer solution.

In conclusion, it was demonstrated that secondary oxidizing agents produced from the reaction between ClO_2 and bromide and iodide ions damage the RO membrane polyamide active layer through halogenation, although ClO_2 does not appear to directly react with the polyamide active layer. However, the mechanism for polyamide oxidation by secondary oxidation agents produced from ClO_2 reaction with bromide and iodide remain unclear. Additional studies on this

topic should elucidate ClO_2-mediated membrane deterioration mechanism and enhance development of RO membranes with high resistance to disinfectants including ClO_2.

REFERENCES

Agus, E. (2009). Disinfection by-products and their potential impact on the quality of water produced by desalination systems: A literature review. Desalination, 237(1-3), 214-237.

Aieta, E M. (1986). A review of chlorine dioxide in drinking water treatment. Journal - American Water Works Association, 78(6), 62-72.

Alayemieka, E. (2012). Modification of polyamide membrane surface with chlorine dioxide solutions of differing ph. Desalination and water treatment, 45(1-3), 84-90.

Antony, A., Fudianto, R., Cox, S., & Leslie, G. (2010). Assessing the oxidative degradation of polyamide reverse osmosis membrane—Accelerated ageing with hypochlorite exposure. Journal Of Membrane Science, 347(1/2), 159-164.

Bartels, C R. (1989). A surface science investigation of composite membranes. Journal of membrane science, 45(3), 225-245.

Belluati, M, Danesi, E, Petrucci, G, et al. (2007). Chlorine dioxide disinfection technology to avoid bromate formation in desalinated seawater in potable waterworks. Desalination, 203(1-3), 312-318.

Bichsel, Y. (2000). Hypoiodous acid: Kinetics of the buffer-catalyzed disproportionation. Water research, 34(12), 3197-3203.

Bray WC (1906). Beitrage zur Kenntnis der Halogensauerstuff verbindungen. Abhandlung III. Zur Kenntnis des Chlordioxyds. Zeitschrift für Physikalische Chemie, 54, 575–581.

Avlonitis, S. (1992). Chlorine degradation of aromatic polyamides. Desalination, 85(3), 321-334.

Chee Meng, P., Peiying, H., Hulling, G., & Wen-Tso, L. (2005). Biofilm Formation Characteristics of Bacterial Isolates Retrieved from a Reverse Osmosis Membrane. Environmental Science & Technology, 39(19), 7541-7550

Coronell, O., Mariñas, B. J., Xijing, Z., & Cahill, D. G. (2008). Quantification of Functional Groups and Modeling of Their Ionization Behavior in the Active Layer of FT30 Reverse Osmosis Membrane. Environmental Science & Technology, 42(14), 5260-5266.

Coronell, O, Mariñas, B J, & Cahill, D G. (2011). Depth heterogeneity of fully aromatic polyamide active layers in reverse osmosis and nanofiltration membranes. Environmental science & technology, 45(10), 4513-4520.

Eigen, M. (1962). The kinetics of halogen hydrolysis. Journal of the American Chemical Society, 84(8), 1355-1361.

Ejike, E N. (2007). Comparative studies of diffusion and permeability of synthetic membrane for buffer solutions. European Journal of Scientific Research, 17(2), 232-235.

Fábián, I. "The Kinetics and Mechanism of the Chlorine Dioxide - Iodide Ion Reaction." Inorganic chemistry 36.12 (1997):2494-2497.

Fickert, S. (1999). Activation of Br2 and BrCl via uptake of HOBr onto aqueous salt solutions. Journal of geophysical research, 104(D19), 23719-23727.

Fukutomi, H. (1967). Kinetic study of the reaction between chlorine dioxide and potassium iodide in aqueous solution. Journal of the American Chemical Society, 89(6), 1362-1366.

Furman, C S. (1998). Mechanism of chlorine dioxide and chlorate ion formation from the reaction of hypobromous acid and chlorite ion. Inorganic chemistry, 37(17), 4321-4327.

Gabelich, C J, Frankin, J, Gerrringer, F, et al. (2005). Enhanced oxidation of polyamide membranes using monochloramine and ferrous iron. Journal of membrane science, 258(1-2), 64-70.

Gazda, M. (1994). Reactions of monochloramine with Br2, Br3 -, HOBr, and OBr-: Formation of bromochloramines. Inorganic chemistry, 33(1), 118-123.

Glater, J. (1981). Effect of halogens on the performance and durability of reverse-osmosis membranes. In Synthetic membranes. (pp. 171-190).American Chemical Society.

Glater, J. (1981). Halogen interactions with typical reverse osmosis membranes. In Proceedings - Water reuse symposium. (pp. 1399-1409).

Glater, J. (1983). Reverse osmosis membrane sensitivity to ozone and halogen disinfectants. Desalination, 48(1), 1-16.

Hayduk, W, & Laudie, H. (1974). Prediction of diffusion coefficients for nonelectrolytes in dilute aqueous solutions. AIChE journal, 20(3), 611-615.

Heijne, G. (1973). Kinetics of the decomposition of aqueous chlorine dioxide solutions. Acta chemica Scandinavica, 27(10), 4018-4019.

Hoigne, J, Hoigné, J, & Bader, H. (1994). Kinetics of reactions of chlorine dioxide (oclo) in water—i. rate constants for inorganic and organic compounds. Water research, 28(1), 45-55.

Junli, H, Huang, J, Wang, Li, et al. (1997). Disinfection effect of chlorine dioxide on bacteria in water. Water research, 31(3), 607-613.

Kang, G, Gao, C, Chen, W, et al. (2007). Study on hypochlorite degradation of aromatic polyamide reverse osmosis membrane. Journal of membrane science, 300(1-2), 165-171.

Kwon, Y, Joksimovic, R, Kim, I, et al. (2011). Effect of bromide on the chlorination of a polyamide membrane. Desalination, 280(1-3), 80-86.

Lengyel, I, Li, J, Kustin, K, et al. (1996). Journal of the American Chemical Society, 118(15), 3708-3719.

Matthiasson, E, & Sivik, B. (1980). Concentration polarization and fouling, Desalination, Volume 35(1), 59-103.

Meng, F., Chae, S., Drews, A., Kraume, M., Shin, H., & Yang, F. (2009). Recent advances in membrane bioreactors (MBRs): Membrane fouling and membrane material. Water Research, 43(6), 1489-1512.

Mi, B, Coronell, O, Marinas, B, et al. (2006). Physico-chemical characterization of nf/ro membrane active layers by rutherford backscattering spectrometry. Journal of membrane science, 282(1-2), 71-81.

Mi, B, Mariñas, B J, & Cahill, D G. (2007). Rbs characterization of arsenic(iii) partitioning from aqueous phase into the active layers of thin-film composite nf/ro membranes. Environmental science & technology, 41(9), 3290-3295.

Odeh, I N, Francisco, J S, & Margerum, D W. (2002). New pathways for chlorine dioxide decomposition in basic solution. Inorganic chemistry, 41(24), 6500-6506.

Petersen, R J. (1993). Composite reverse osmosis and nanofiltration membranes. Journal of membrane science, 83(1), 81-150.

Saenz De Jubera, A.M., Saenz de Jubera, Gao, Y, et al. (2012). Enhancing the performance of nanofiltration membranes by modifying the active layer with aramide dendrimers. Environmental science & technology, 46(17), 9592-9599.

Saenz De Jubera, A.M., Saenz de Jubera, Herbison, J H, et al. (2013). Development and performance characterization of a polyamide nanofiltration membrane modified with covalently bonded aramide dendrimers. Environmental science & technology, 47(15), 8642-8649.

Sander, R. (1999). Compilation of Henry's law constants for inorganic and organic species of potential importance in environmental chemistry, 9.

Sandín, R, Ferrero, E, Repollés, C, et al. (2013). Reverse osmosis membranes oxidation by hypochlorite and chlorine dioxide: Spectroscopic techniques vs. fujiwara test. Desalination and water treatment, 51(1-3), 318-327.

Soulard, M, Bloc, F, & Hatterer, A. (1981). Diagrams of existence of chloramines and bromamines in aqueous solution. Journal of the Chemical Society. Dalton transactions, (12), 2300-2310.

Silva, M., Tessaro, I., & Wada, K. (2006). Investigation of oxidative degradation of polyamide reverse osmosis membranes by monochloramine solutions. Journal Of Membrane Science, 282(1/2), 375-382.

Singh, R. (1994). Polyamide polymer solution behaviour under chlorination conditions. Journal of membrane science, 88(2-3), 285-287.

Sourirajan, S, & Kucera, J. (1970). Reverse osmosis : Design, processes, and applications for engineers. Hoboken: John Wiley & Sons, Inc..

Suzuki, T, Lu, Y, Zhang, W, et al. (2007). Performance characterization of nanofiltration membranes based on rigid star amphiphiles. Environmental science & technology, 41(17), 6246-6252.

Rav-Acha Ch.. (1985). Disinfection of drinking water rich in bromide with chlorine and chlorine dioxide, while minimizing the formation of undesirable by-products. Water science and technology, 17(4-5 -5 pt 2), 611-621.

Richardson, S D. (2000). Identification of new drinking water disinfection by-products from ozone, chlorine dioxide, chloramine, and chlorine. Water, air and soil pollution, 123(1-4), 95-102.

Tzanavaras, P D, Themelis, D G, & Kika, F S. (2007). Review of analytical methods for the determination of chlorine dioxide. Central European Journal of Chemistry, 5(1), 1-12.

Urama, R I. (1997). Mechanistic interpretation of solute permeation through a fully aromatic polyamide reverse osmosis membrane. Journal of membrane science, 123(2), 267-280.

Vicuña Reyes, J P, Luh, J, & Mariñas, B J. (2008). Inactivation of mycobacterium avium with chlorine dioxide. Water research, 42(6-7), 1531-1538.

Wijmans, J G, & Baker, R W. (1995). The solution-diffusion model: A review. Journal of membrane science, 107(1-2), 1-21.

TABLES AND FIGURES

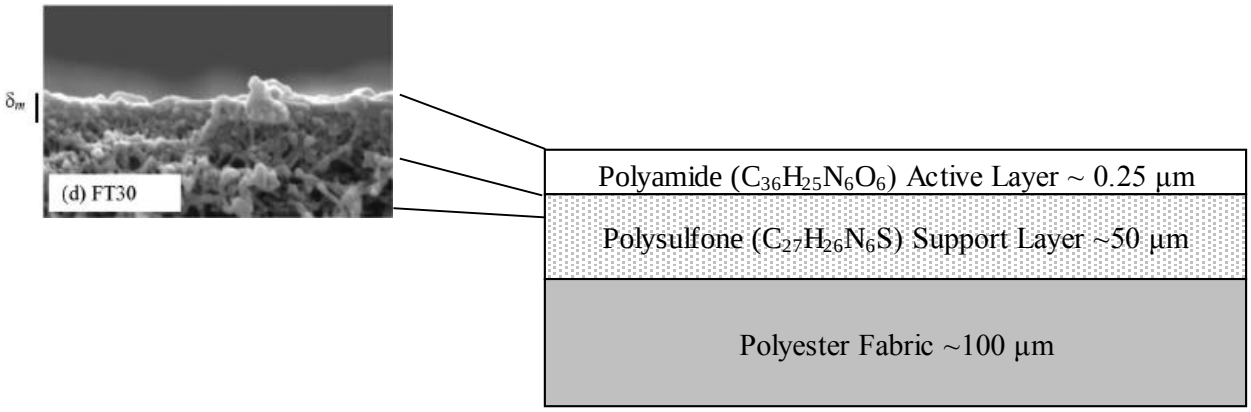

Figure 1. SEM and Schematic and images of a membrane cross-section. SEM image adapted from Mi et al. 2006. δ_m represents the thickness of polyamide active layer.

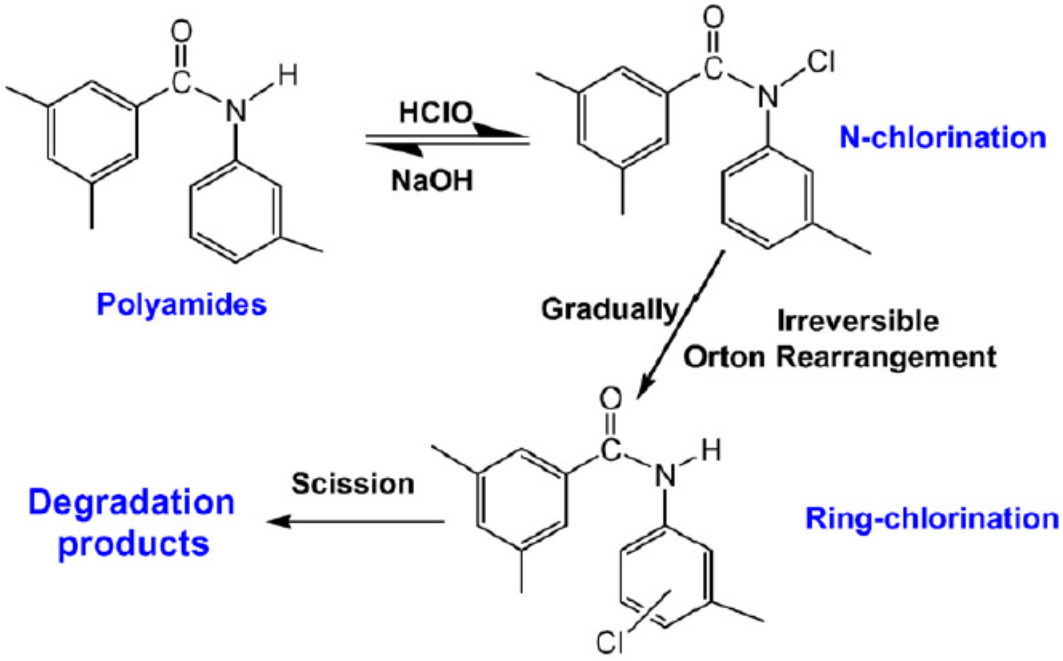

Figure 2. Polyamide degradation process with hypochloride. First, N-chlorination is proceeded when hypochlorite exists. Then, since the N-chlorinated amides have limited stability, ring chlorination can occur via irreversible Orton Rearrangement (Kang et al., 2007).

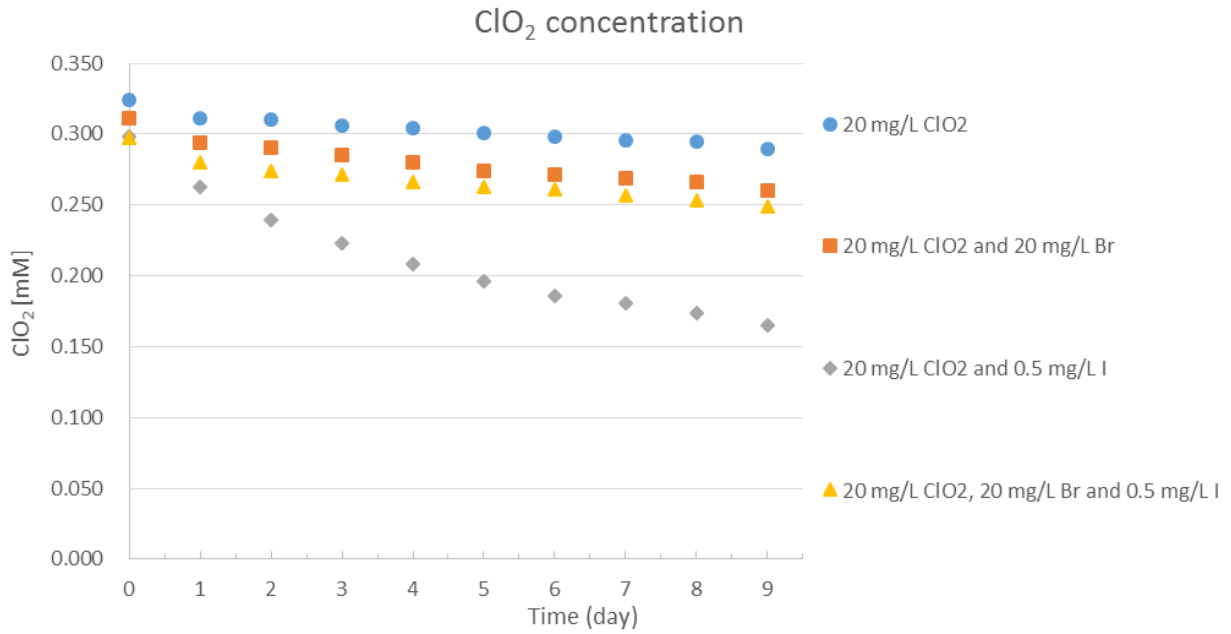

Figure 3. ClO_2 concentration profile over time. Diamonds, square, triangle, and circle plots represent no compounds, 0.5 mg/L I, 20 mg/L, 0.5 mg/L I and 20 mg/L Br disinfected with approximately 20 mg/L ClO_2 (0.30 mM), respectively. pH was set as 7.5 with 10 mM phosphate buffer solution.

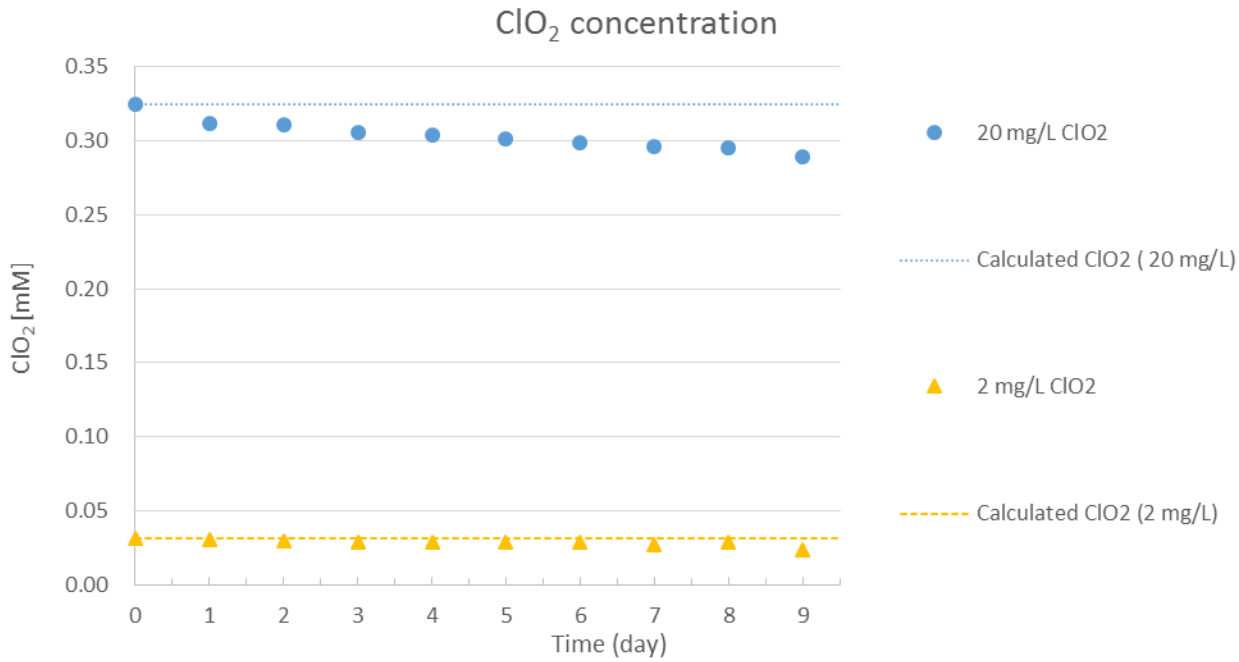

Figure 4. Raw data and calculated ClO_2 concentration profile over time. Circle and triangle plots represent 20 mg/L ClO_2 and 2 mg/L ClO_2, respectively. Small and large dotted line indicates calculated 20 mg/L ClO_2 and 2 mg/L ClO_2 based on eq (2), respectively. pH was set as 7.5 with 10 mM phosphate buffer solution.

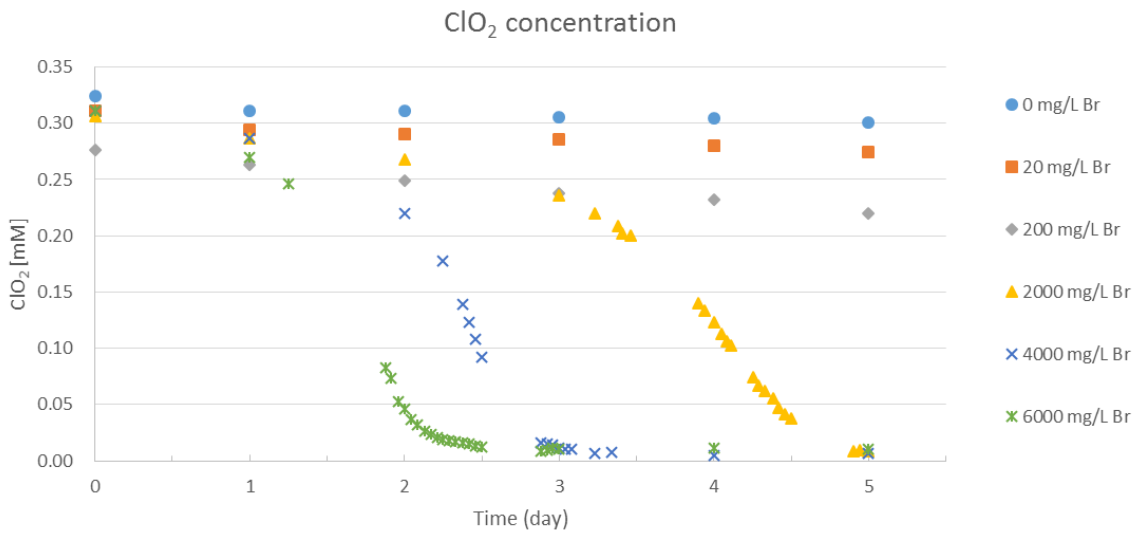

Figure 5. ClO_2 concentration profile over time. Circle, square, Diamonds, triangle, cross and asterisk plots represent no compounds, 20 mg/L Br, 200 mg/L, 2000 mg/L Br, 4000 mg/L Br and 6000 mg/L Br disinfected with approximately 20 mg/L ClO_2 (0.30 mM), respectively. pH was set as 7.5 with 10 mM phosphate buffer solution.

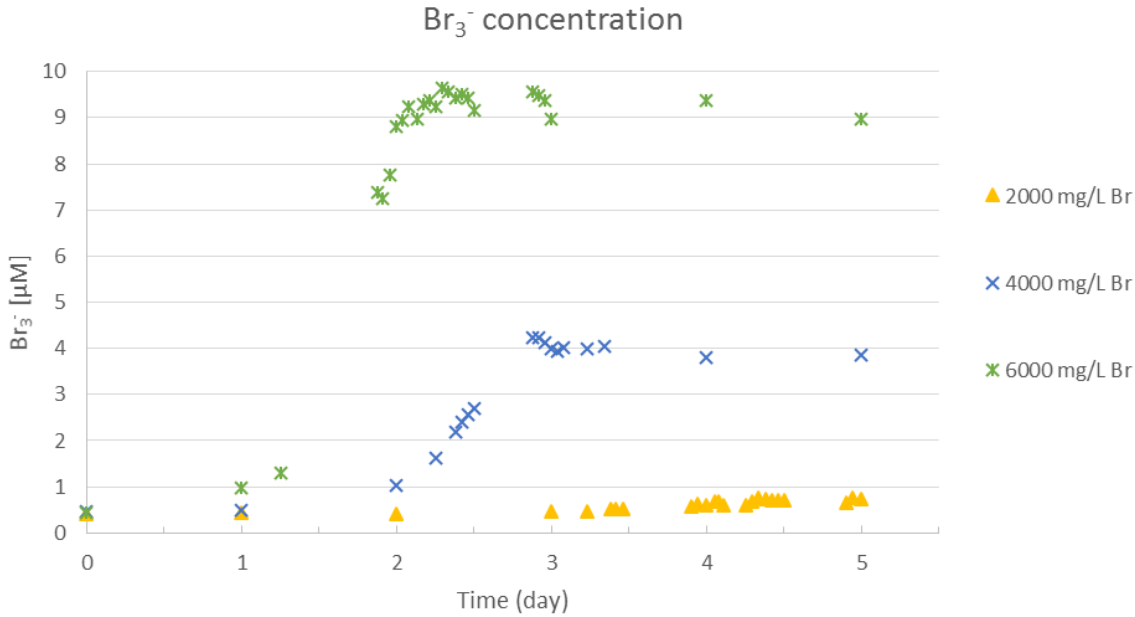

Figure 6. Br_3^- concentration profile over time. Triangle, cross and asterisk plots represent, 2000 mg/L Br, 4000 mg/L Br and 6000 mg/L Br disinfected with approximately 20 mg/L ClO_2 (0.30 mM), respectively. pH was set as 7.5 with 10 mM phosphate buffer solution.

Table 1. Bromide and bromine compounds concentration at equilibrium. Br_3^- concentration was calculated by UV absorbance and eq. (6) with Br_3^- molar absorptivity (35000 L M^{-1} cm^{-1}). Br_2 and HOBr were calculated by eq. (16) and eq. (23), respectively. Experimental conditions correspond to approximately 20 mg/L ClO_2 with 2000 mg/L Br, 4000 mg/L Br and 6000 mg/L Br, respectively. pH was set as 7.5 with 10 mM phosphate buffer solution.

Br^-		Br_3^-	Br_2	HOBr
mg/L Br	[mM]	[μM]	[μM]	[μM]
2000	25.03	0.77	1.86	16.13
4000	50.06	4.23	5.09	22.10
6000	75.09	9.66	7.75	22.43

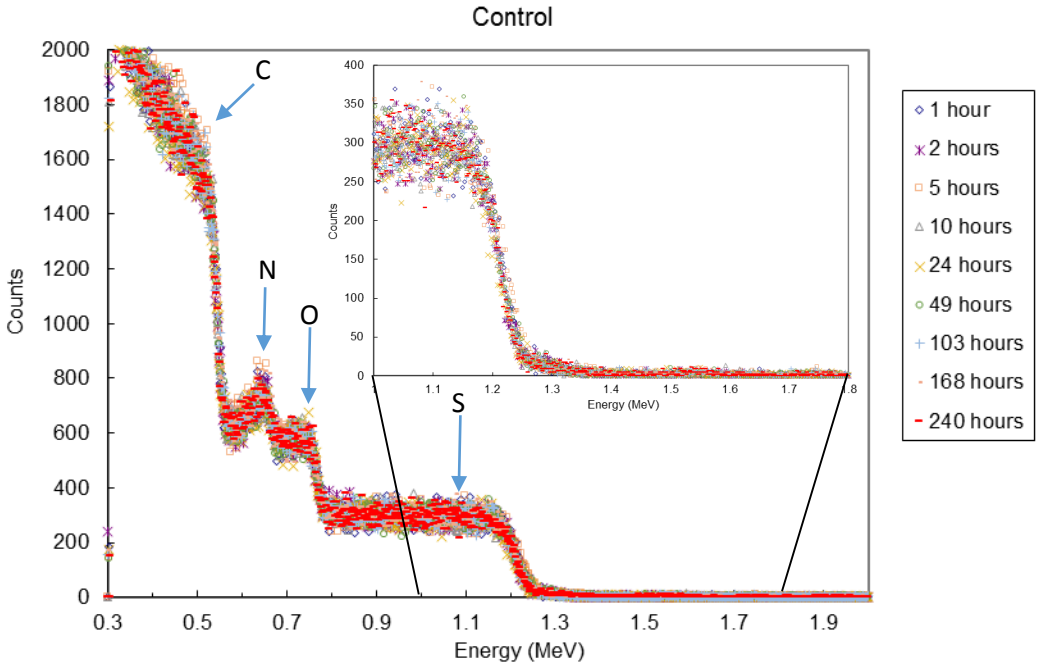

Figure 7. RBS characterization after SW30HR membrane exposure to 10 mM phosphate. Data points obtained using SIMNRA based on RBS analysis data.

Table 2. Atomic concentration (atoms element/atoms PA) data from membrane exposure to 10mM phosphate.

atomic (atoms element/atoms PA)									
hour	Layer thickness [atoms/cm2]	%C	%O	%N	%H	%K	%Cl	%I	%Br
1	810	41.0%	7.4%	6.9%	44.6%	0.017%	0.100%	0.0000%	0.0000%
2	840	41.0%	7.5%	6.9%	44.5%	0.020%	0.100%	0.0000%	0.0000%
5	790	41.0%	7.3%	6.9%	44.7%	0.030%	0.080%	0.0000%	0.0000%
10	810	41.0%	7.5%	6.9%	44.5%	0.020%	0.110%	0.0000%	0.0000%
24	840	41.0%	7.9%	6.2%	44.8%	0.030%	0.080%	0.0000%	0.0000%
49	800	43.0%	7.5%	6.8%	42.6%	0.020%	0.090%	0.0000%	0.0000%
103	840	43.0%	7.5%	6.2%	43.2%	0.030%	0.080%	0.0000%	0.0000%
168	840	44.0%	7.7%	6.7%	41.5%	0.020%	0.100%	0.0000%	0.0000%
240	840	41.0%	7.5%	6.9%	44.5%	0.040%	0.080%	0.0000%	0.0000%

Table 3. Concentration data by weight (g element/g PA) from membrane exposure to 10mM phosphate.

weight (g element/g PA) without the ion							
hour	denominator=Σ（εi × Mi）	%C	%O	%N	%H	%K	%Cl
1	7.56E+00	65.10%	15.67%	12.78%	5.90%	0.09%	0.47%
2	7.57E+00	64.96%	15.84%	12.75%	5.87%	0.10%	0.47%
5	7.54E+00	65.24%	15.49%	12.81%	5.93%	0.16%	0.38%
10	7.58E+00	64.93%	15.84%	12.75%	5.87%	0.10%	0.52%
24	7.54E+00	65.25%	16.76%	11.51%	5.94%	0.16%	0.38%
49	7.78E+00	66.34%	15.43%	12.24%	5.48%	0.10%	0.41%
103	7.70E+00	67.01%	15.58%	11.27%	5.61%	0.15%	0.37%
168	7.91E+00	66.77%	15.58%	11.86%	5.25%	0.10%	0.45%
240	7.57E+00	64.95%	15.84%	12.75%	5.87%	0.21%	0.37%

Table 4. Concentration data by weight (g element/g PA) and by volume (g element/L PA) from membrane exposure to 10mM phosphate.

molar concentration								
hour	[mol I /g PA]	[mol Br /g PA]	[mol K /g PA]	[mol Cl /g PA]	mol I/L	mol Br/L	mol K/L	mol Cl/L
1	0.00E+00	0.00E+00	1.37E−05	8.09E−05	0.000	0.00	0.02	0.10
2	0.00E+00	0.00E+00	1.62E−05	8.08E−05	0.000	0.00	0.02	0.10
5	0.00E+00	0.00E+00	2.43E−05	6.48E−05	0.000	0.00	0.03	0.08
10	0.00E+00	0.00E+00	1.61E−05	8.88E−05	0.000	0.00	0.02	0.11
24	0.00E+00	0.00E+00	2.42E−05	6.46E−05	0.000	0.00	0.03	0.08
49	0.00E+00	0.00E+00	1.62E−05	7.27E−05	0.000	0.00	0.02	0.09
103	0.00E+00	0.00E+00	2.43E−05	6.47E−05	0.000	0.00	0.03	0.08
168	0.00E+00	0.00E+00	1.61E−05	8.05E−05	0.000	0.00	0.02	0.10
240	0.00E+00	0.00E+00	3.23E−05	6.46E−05	0.000	0.00	0.04	0.08

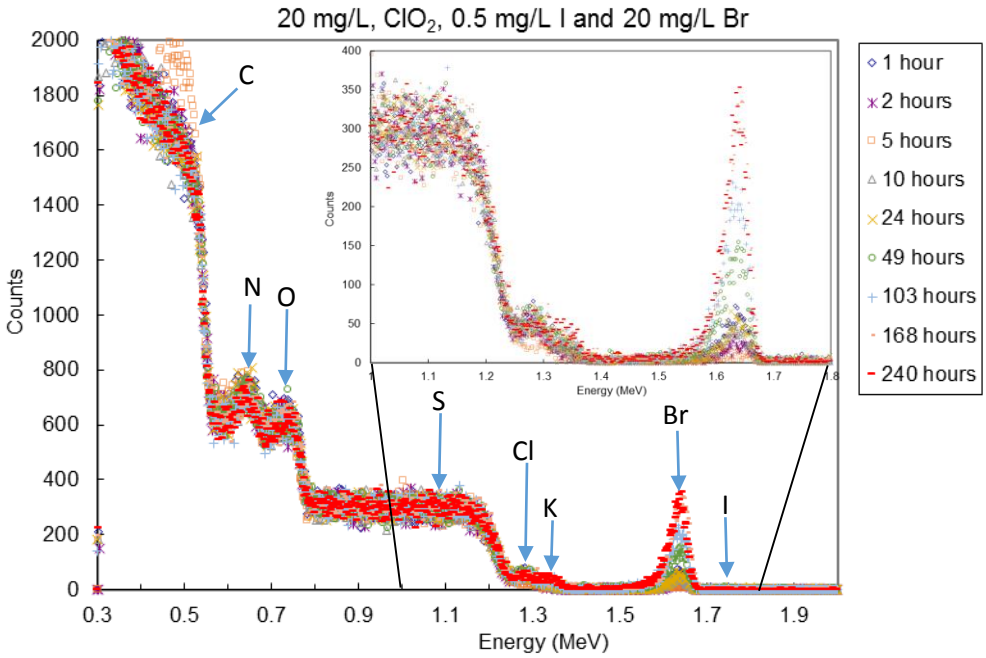

Figure 8. RBS characterization after SW30HR membrane exposure to 20 mg/L Br and 0.5 mg/L I disinfected with 20 mg/L ClO_2. Data points obtained using SIMNRA based on RBS analysis data.

Table 5. Atomic concentration (atoms element/atoms PA) data from membrane exposure to 20 mg/L Br and 0.5 mg/L I disinfected with 20 mg/L ClO_2.

atomic (atoms element/atoms PA)									
hour	Layer thickness [atoms/cm2]	%C	%O	%N	%H	%K	%Cl	%I	%Br
1	830	42.0%	8.8%	6.8%	41.8%	0.050%	0.440%	0.0040%	0.0900%
2	800	43.0%	8.3%	6.8%	41.5%	0.040%	0.320%	0.0030%	0.0360%
5	800	47.0%	7.8%	6.8%	38.1%	0.020%	0.280%	0.0030%	0.0250%
10	860	40.0%	8.4%	6.4%	44.7%	0.030%	0.420%	0.0040%	0.0590%
24	830	42.0%	8.6%	6.3%	42.6%	0.070%	0.370%	0.0030%	0.0780%
49	820	41.0%	8.9%	6.8%	42.6%	0.110%	0.390%	0.0040%	0.2200%
103	820	40.0%	8.9%	6.0%	44.3%	0.120%	0.350%	0.0030%	0.3200%
168	830	40.0%	8.9%	6.0%	44.1%	0.150%	0.350%	0.0050%	0.5000%
240	800	42.0%	8.6%	6.0%	42.4%	0.150%	0.310%	0.0015%	0.5000%

Table 6. Concentration data by weight (g element/g PA) from membrane exposure to 20 mg/L Br and 0.5 mg/L I disinfected with 20 mg/L ClO_2.

weight (g element/g PA) without the ion							
hour	denominator=Σ（εi × Mi）	%C	%O	%N	%H	%K	%Cl
1	7.99E+00	63.05%	17.61%	11.91%	5.23%	0.24%	1.95%
2	7.98E+00	64.63%	16.63%	11.92%	5.20%	0.20%	1.42%
5	8.33E+00	67.72%	14.99%	11.43%	4.57%	0.09%	1.19%
10	7.65E+00	62.76%	17.57%	11.72%	5.84%	0.15%	1.95%
24	7.88E+00	63.94%	17.46%	11.19%	5.40%	0.35%	1.67%
49	7.90E+00	62.25%	18.02%	12.05%	5.39%	0.54%	1.75%
103	7.68E+00	62.51%	18.55%	10.94%	5.77%	0.61%	1.62%
168	7.69E+00	62.44%	18.52%	10.93%	5.74%	0.76%	1.62%
240	7.85E+00	64.21%	17.53%	10.70%	5.41%	0.75%	1.40%

Table 7. Concentration data by weight (g element/g PA) and by volume (g element/L PA) from membrane exposure to 20 mg/L Br and 0.5 mg/L I disinfected with 20 mg/L ClO_2.

molar concentration								
hour	[mol I /g PA]	[mol Br /g PA]	[mol K /g PA]	[mol Cl /g PA]	mol I/L	mol Br/L	mol K/L	mol Cl/L
1	3.10E-06	6.98E-05	3.88E-05	3.41E-04	0.004	0.09	0.05	0.42
2	2.36E-06	2.83E-05	3.14E-05	2.52E-04	0.003	0.04	0.04	0.31
5	2.38E-06	1.98E-05	1.58E-05	2.22E-04	0.003	0.02	0.02	0.27
10	3.13E-06	4.61E-05	2.34E-05	3.28E-04	0.004	0.06	0.03	0.41
24	2.34E-06	6.09E-05	5.46E-05	2.89E-04	0.003	0.08	0.07	0.36
49	3.09E-06	1.70E-04	8.51E-05	3.02E-04	0.004	0.21	0.11	0.37
103	2.33E-06	2.49E-04	9.32E-05	2.72E-04	0.003	0.31	0.12	0.34
168	3.87E-06	3.87E-04	1.16E-04	2.71E-04	0.005	0.48	0.14	0.34
240	1.17E-06	3.89E-04	1.17E-04	2.41E-04	0.001	0.48	0.14	0.30

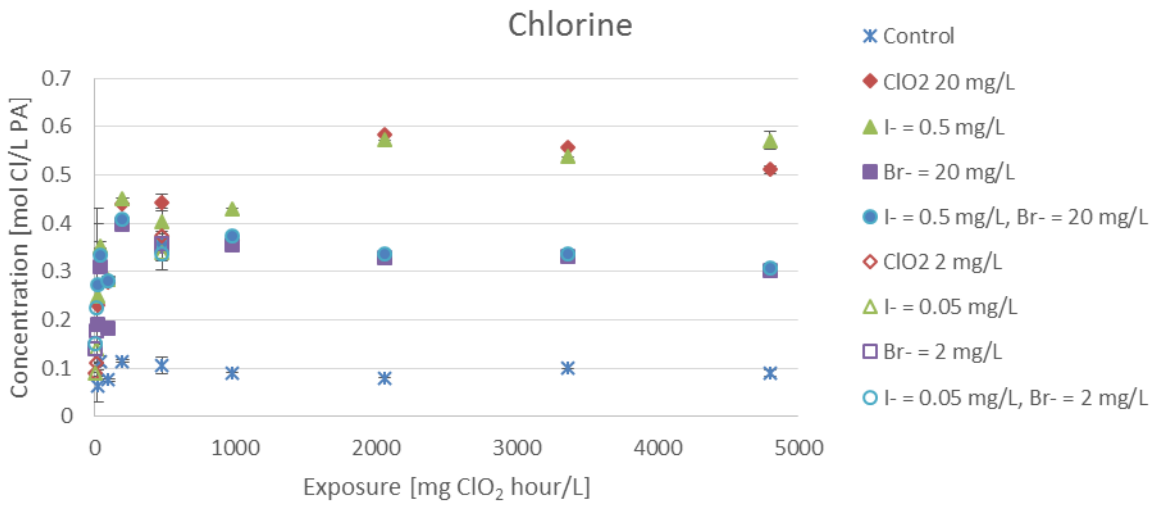

Figure 9. Chlorine concentration profile in the PA membrane over time. Asterisk plots represent the control solution without ClO_2, solid fill plots of Diamonds, triangle, square and circle represent no compounds, 0.5 mg/L I, 20 mg/L, 0.5 mg/L I and 20 mg/L Br disinfected with 20 mg/L ClO_2, respectively. No solid fill plots of Diamonds, triangle, square and circle represent no compounds, 0.05 mg/L I, 2 mg/L, 0.05 mg/L I and 2 mg/L Br disinfected with 2 mg/L ClO_2, respectively. All solutions set pH 7.5 with 10mM phosphate buffer solution. X axis indicates the ClO_2 exposure time (ClO_2 concentration (mg/L) × soaking time).

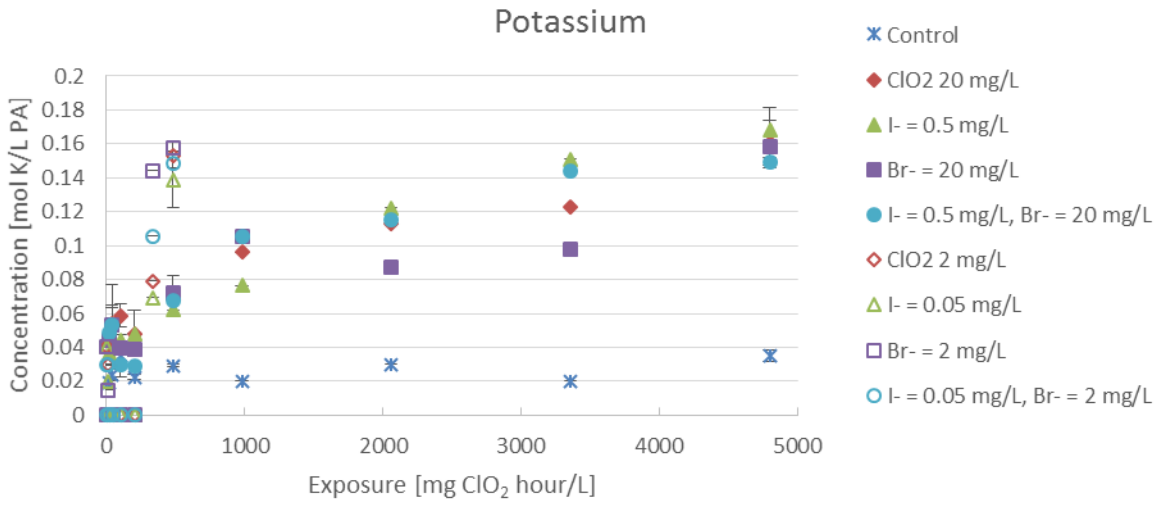

Figure 10. Potassium concentration profile in the PA membrane over time. Asterisk plots represent the control solution without ClO_2, closed plots of Diamonds, triangle, square and circle represent no compounds, 0.5 mg/L I, 20 mg/L, 0.5 mg/L I and 20 mg/L Br disinfected with 20 mg/L ClO_2, respectively. Open plots of Diamonds, triangle, square and circle represent no compounds, 0.05 mg/L I, 2 mg/L, 0.05 mg/L I and 2 mg/L Br disinfected with 2

mg/L ClO_2, respectively. All solutions set pH 7.5 with 10mM phosphate buffer solution. X axis indicates the ClO_2 exposure time (ClO_2 concentration (mg/L) × soaking time).

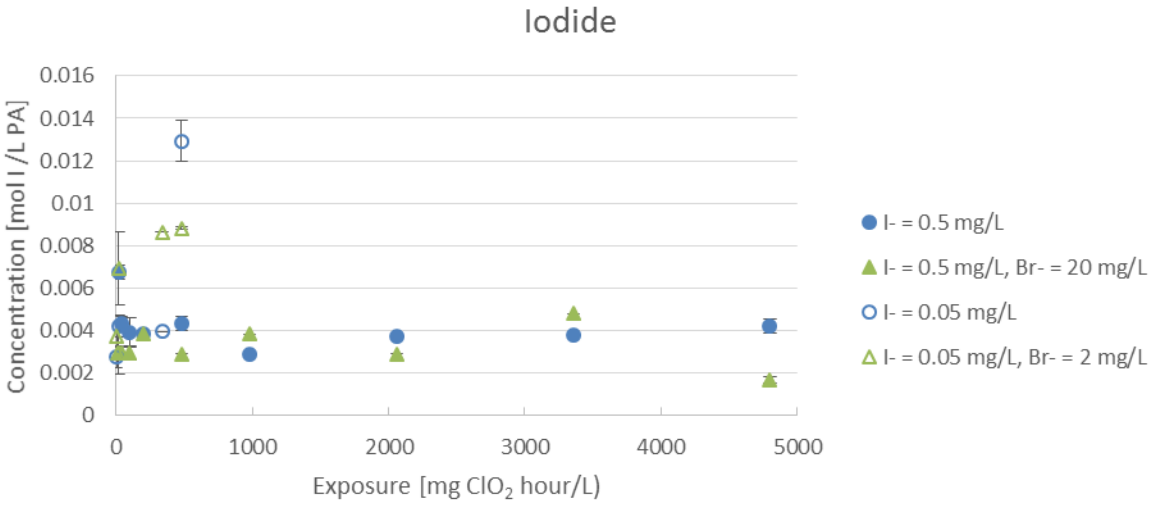

Figure 11. Iodide concentration profile in the PA membrane over time. Closed plots of circle and triangle represent 0.5 mg/L I, 0.5 mg/L I and 20 mg/L Br disinfected with 20 mg/L ClO_2, respectively. Open plots of circle and triangle represent 0.05 mg/L I, 0.05 mg/L I and 2 mg/L Br disinfected with 2 mg/L ClO_2, respectively. All solutions set pH 7.5 with 10mM phosphate buffer solution. X axis indicates the ClO_2 exposure time (ClO_2 concentration (mg/L) × soaking time).

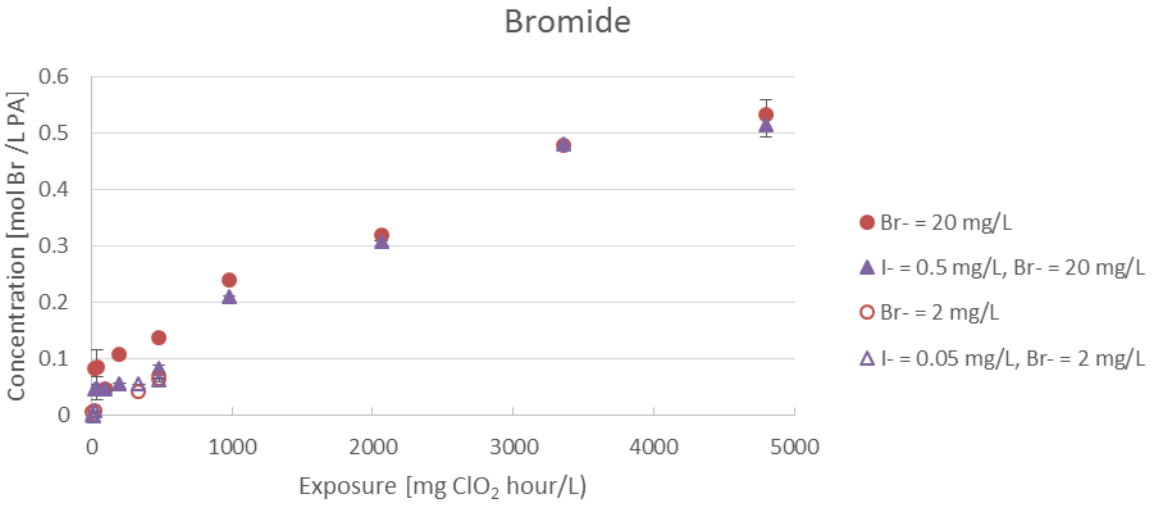

Figure 12. Bromide concentration profile in the PA membrane over time. Closed plots of circle and triangle represent 2 mg/L Br, 0.5 mg/L I and 2 mg/L Br disinfected with 2 mg/L ClO_2, respectively. Open plots of circle and triangle represent 2 mg/L Br, 0.5 mg/L I and 2 mg/L Br disinfected with 2 mg/L ClO_2, respectively. All solutions set pH 7.5 with 10mM phosphate buffer solution. X axis indicates the ClO_2 exposure time (ClO_2 concentration (mg/L) × soaking time).

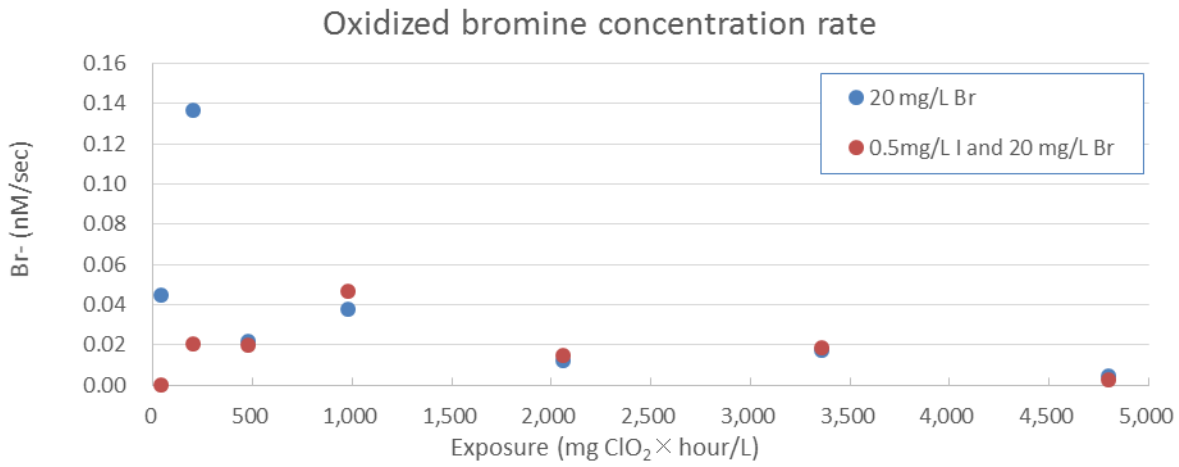

Figure 13. the oxidized bromine concentration rate profile over time. Br- (nM/sec) was calculated by eq. (16) anf (17). The mean value of oxidized bromine concentration rates were 0.045 (nM/sec) at 20 mg/L Br and 0.015 (nM/sec) at 0.5mg/L I and 20 mg/L Br, respectively.

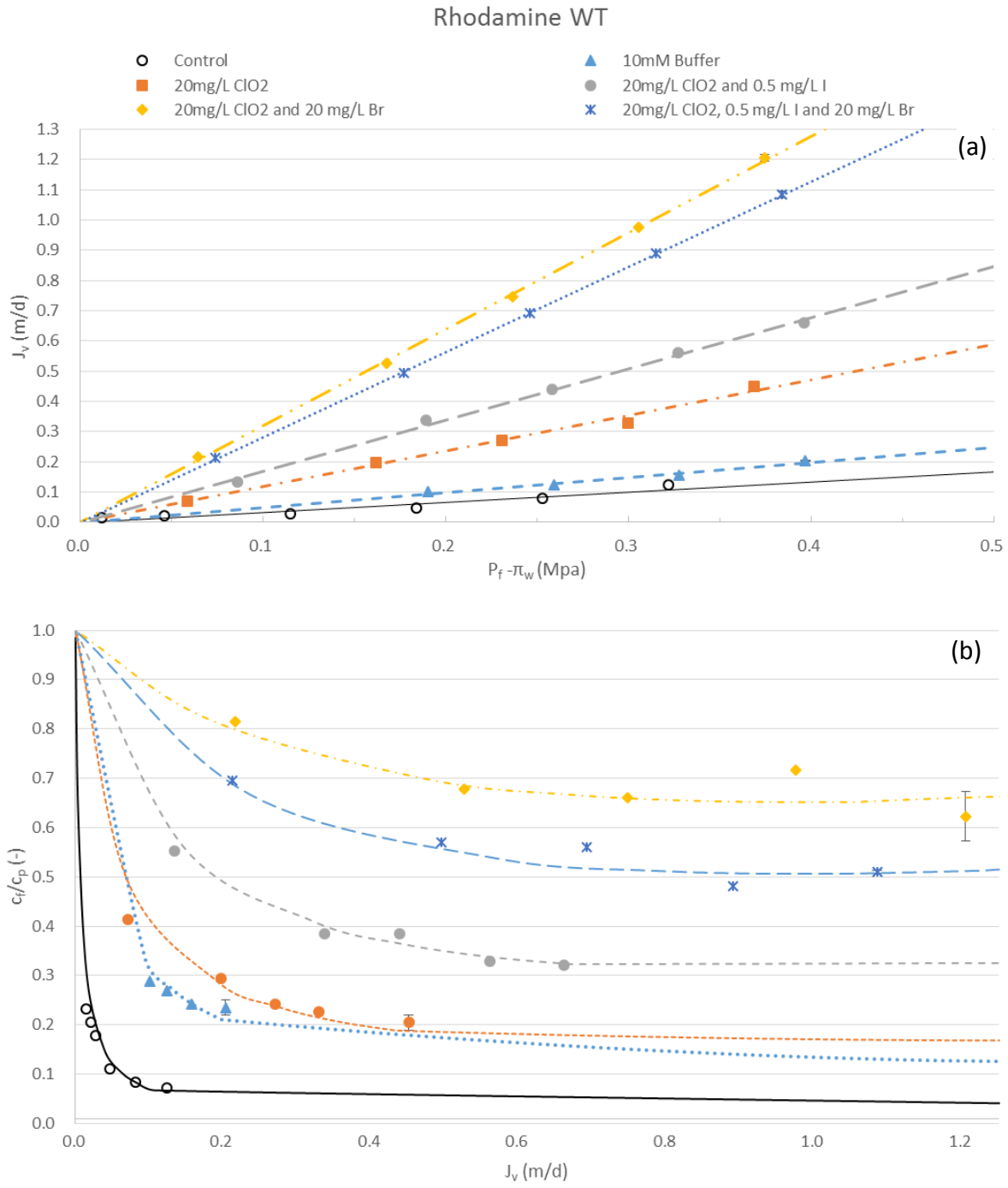

Figure 14. Experimental (symbols) and fitted (lines) (a) water permeability and (b) solute passage for Rhodamine WT rejection experiments. Opened circle represents the pure RO membrane exposure to nanopure water at least 24 hours, closed triangle represents the RO membrane exposure to 10 mM phosphate buffer solution at pH 7.5 for 10 days, closed square, closed circle closed Diamonds and asterisk represent RO membranes exposure to no compounds, 0.5 mg/L I, 20 mg/L Br, 0.5 mg/L I and 20 mg/L Br, disinfected with 20 mg/L ClO2 with 10 mM phosphate buffer solution at pH 7.5 for 10 days, respectively.

Table 8. Permeation coefficients of Rhodamine WT.

Membrane	Solute	π_w	A_D	B	α	k
		Mpa	m/d/Mpa	m/d	–	m/d
Control	Rhodamine WT	0.092	0.32	0.004	0.045	20
10mM Buffer	Rhodamine WT	0.017	0.41	0.017	0.167	
20mg/L ClO_2	Rhodamine WT	0.045	0.99	0.031	0.160	
20mg/L ClO_2 and 0.5 mg/L I^-	Rhodamine WT	0.017	1.32	0.098	0.221	
20mg/L ClO_2 and 20 mg/L Br^-	Rhodamine WT	0.039	1.68	0.203	0.403	
20mg/L ClO_2, 0.5 mg/L I^- and 20 mg/L Br^-	Rhodamine WT	0.030	1.43	0.300	0.552	

APPENDIX A

SUPPLEMENTAL FIGURES AND TABLES OF CHLORINE DIOXIDE REACTIONS

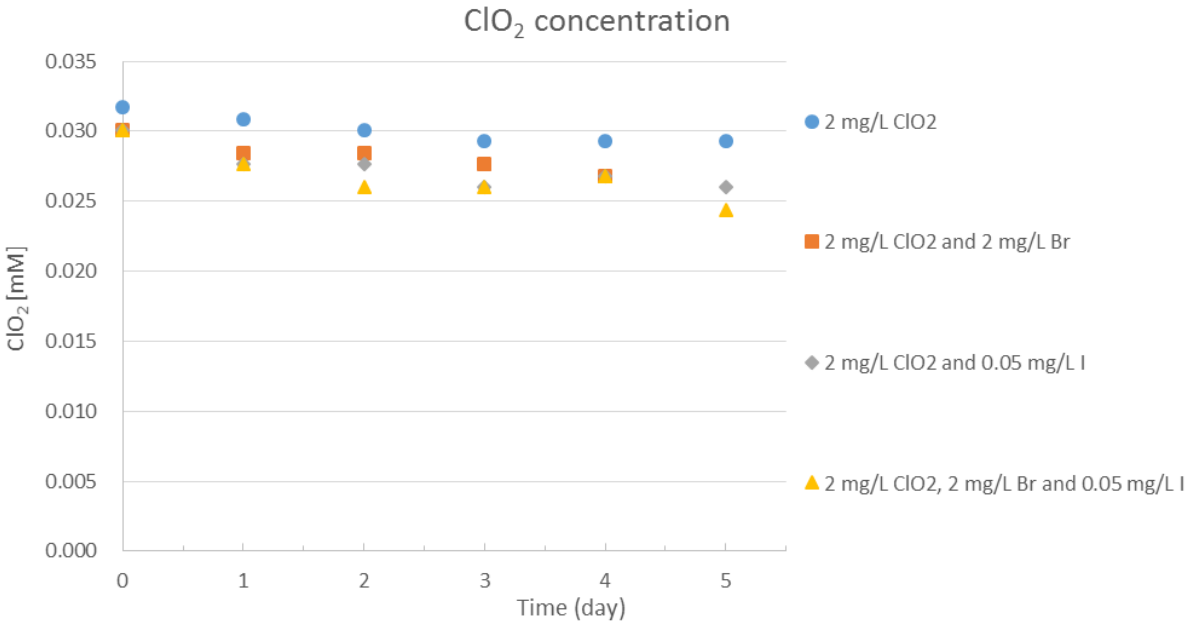

Figure A1. ClO_2 concentration profile over time. Diamond, square, triangle, and circle plots represent no compounds, 0.05 mg/L I, 2 mg/L, 0.5 mg/L I and 2 mg/L Br disinfected with approximately 2 mg/L ClO_2 (0.30 mM), respectively. pH was set as 7.5 with 10 mM phosphate buffer solution.

Table A1. Raw data of UV absorbance (λ= 359 nm) and ClO_2 concentration over time. Experimental conditions correspond to 2 mg/L ClO_2 at pH = 7.5 which was controlled by 10mM phosphate buffer solution. "Calculated ClO_2" was estimated by eq. (2).

2 mg/L ClO_2				
time (day)	ClO_2			Calculated ClO_2
	Absorbance	(mg/L)	[mM]	[mM]
0	0.039	2.14	0.032	0.03170732
1	0.038	2.09	0.031	0.03170728
2	0.037	2.03	0.030	0.03170723
3	0.036	1.98	0.029	0.03170719
4	0.036	1.98	0.029	0.03170715
5	0.036	1.98	0.029	0.03170711
6	0.035	1.92	0.028	0.03170706
7	0.033	1.81	0.027	0.03170702
8	0.035	1.92	0.028	0.03170698

Table A2. Raw data of UV absorbance (λ= 359 nm) and ClO_2 concentration over time. Experimental conditions correspond to 2 mg/L ClO_2 and 2 mg/L Br at pH = 7.5 which was controlled by 10mM phosphate buffer solution.

2 mg/L ClO_2 and 2 mg/L Br			
time (day)	ClO_2		
	Absorbance	(mg/L)	[mM]
0	0.037	2.03	0.030
1	0.035	1.92	0.028
2	0.035	1.92	0.028
3	0.034	1.87	0.028
4	0.033	1.81	0.027

Table A3. Raw data of UV absorbance (λ= 359 nm) and ClO_2 concentration over time. Experimental conditions correspond to 2 mg/L ClO_2 and 0.05 mg/L I at pH = 7.5 which was controlled by 10mM phosphate buffer solution.

2 mg/L ClO_2 and 0.05 mg/L I			
	ClO_2		
time (day)	Absorbance	(mg/L)	[mM]
0	0.037	2.03	0.030
1	0.034	1.87	0.028
2	0.034	1.87	0.028
3	0.032	1.76	0.026
4	0.033	1.81	0.027
5	0.032	1.76	0.026
6	0.032	1.76	0.026
7	0.032	1.76	0.026
8	0.033	1.81	0.027

Table A4. Raw data of UV absorbance (λ= 359 nm) and ClO_2 concentration over time. Experimental conditions correspond to 2 mg/L ClO_2, 2 mg/L Br and 0.05 mg/L I at pH = 7.5 which was controlled by 10mM phosphate buffer solution.

2 mg/L ClO_2, 2 mg/L Br and 0.05 mg/L I			
time (day)	ClO_2		
	Absorbance	(mg/L)	[mM]
0	0.037	2.03	0.030
1	0.034	1.87	0.028
2	0.032	1.76	0.026
3	0.032	1.76	0.026
4	0.033	1.81	0.027
5	0.030	1.65	0.024

Table A5. Raw data of UV absorbance (λ= 359 nm) and ClO_2 concentration over time. Experimental conditions correspond to 20 mg/L ClO_2 at pH = 7.5 which was controlled by 10mM phosphate buffer solution. "Calculated ClO_2" was estimated by eq. (2).

20 mg/L ClO_2				
time (day)	ClO_2			0 mg/L Br Calculated
	Absorbance	(mg/L)	[mM]	mM
0	0.399	21.90	0.324	0.324390
1	0.383	21.02	0.311	0.324386
2	0.382	20.96	0.311	0.324381
3	0.376	20.63	0.306	0.324377
4	0.374	20.52	0.304	0.324373
5	0.37	20.30	0.301	0.324368
6	0.367	20.14	0.298	0.324364
7	0.364	19.98	0.296	0.324359
8	0.363	19.92	0.295	0.324355
9	0.356	19.54	0.289	0.324351

Table A6. Raw data of UV absorbance (λ= 359 nm) and ClO_2 concentration over time. Experimental conditions correspond to 20 mg/L ClO_2 and 20 mg/L Br at pH = 7.5 which was controlled by 10mM phosphate buffer solution.

20 mg/L ClO_2 and 20 mg/L Br			
time (day)	ClO_2		
	Absorbance	(mg/L)	[mM]
0	0.383	21.02	0.311
1	0.362	19.87	0.294
2	0.357	19.59	0.290
3	0.351	19.26	0.285
4	0.344	18.88	0.280
5	0.337	18.49	0.274
6	0.334	18.33	0.272
7	0.331	18.16	0.269
8	0.327	17.95	0.266
9	0.32	17.56	0.260

Table A7. Raw data of UV absorbance (λ= 359 nm) and ClO_2 concentration over time. Experimental conditions correspond to 20 mg/L ClO_2 and 0.5 mg/L I at pH = 7.5 which was controlled by 10mM phosphate buffer solution.

20 mg/L ClO_2 and 0.5 mg/L I			
	ClO_2		
time (day)	Absorbance	(mg/L)	[mM]
0	0.367	20.14	0.298
1	0.323	17.73	0.263
2	0.295	16.19	0.240
3	0.274	15.04	0.223
4	0.256	14.05	0.208
5	0.241	13.23	0.196
6	0.229	12.57	0.186
7	0.222	12.18	0.180
8	0.214	11.74	0.174
9	0.203	11.14	0.165

Table A8. Raw data of UV absorbance (λ= 359 nm) and ClO_2 concentration over time. Experimental conditions correspond to 20 mg/L ClO_2, 20 mg/L Br and 0.5 mg/L I at pH = 7.5 which was controlled by 10mM phosphate buffer solution.

20 mg/L ClO_2, 20 mg/L Br and 0.5 mg/L I			
time (day)	ClO_2		
	Absorbance	(mg/L)	[mM]
0	0.366	20.09	0.298
1	0.344	18.88	0.280
2	0.337	18.49	0.274
3	0.334	18.33	0.272
4	0.327	17.95	0.266
5	0.323	17.73	0.263
6	0.321	17.62	0.261
7	0.316	17.34	0.257
8	0.311	17.07	0.253
9	0.306	16.79	0.249

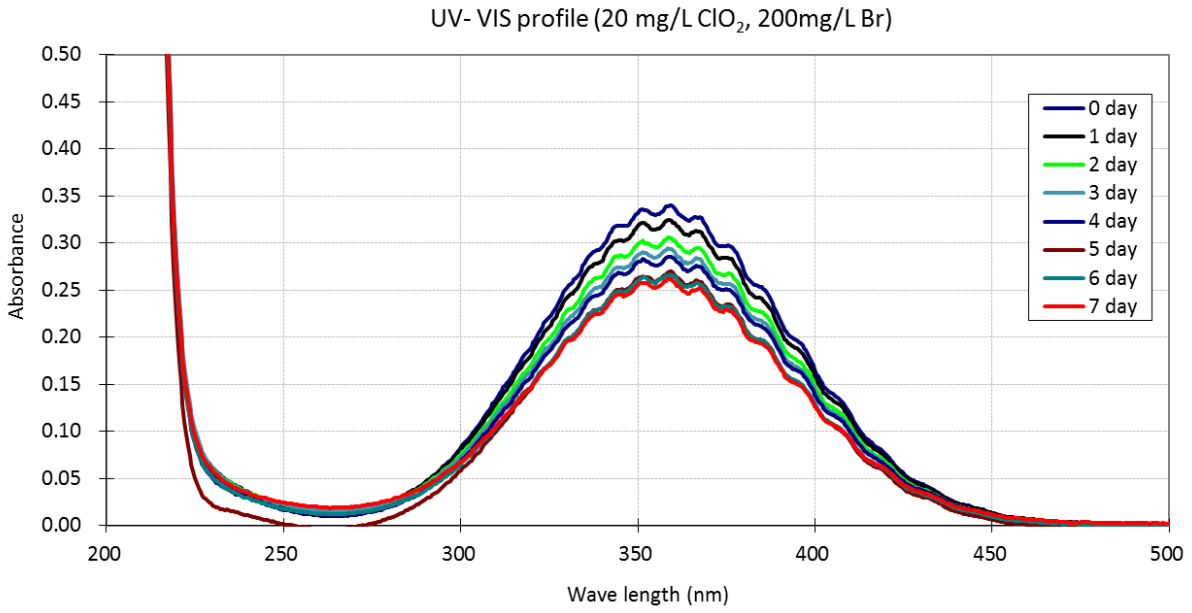

Figure A2. The UV-VIS spectrum over time. Experimental conditions correspond to 200 mg/L Br disinfected with 20 mg/L ClO_2 at pH = 7.5 which was controlled by 10mM phosphate buffer solution.

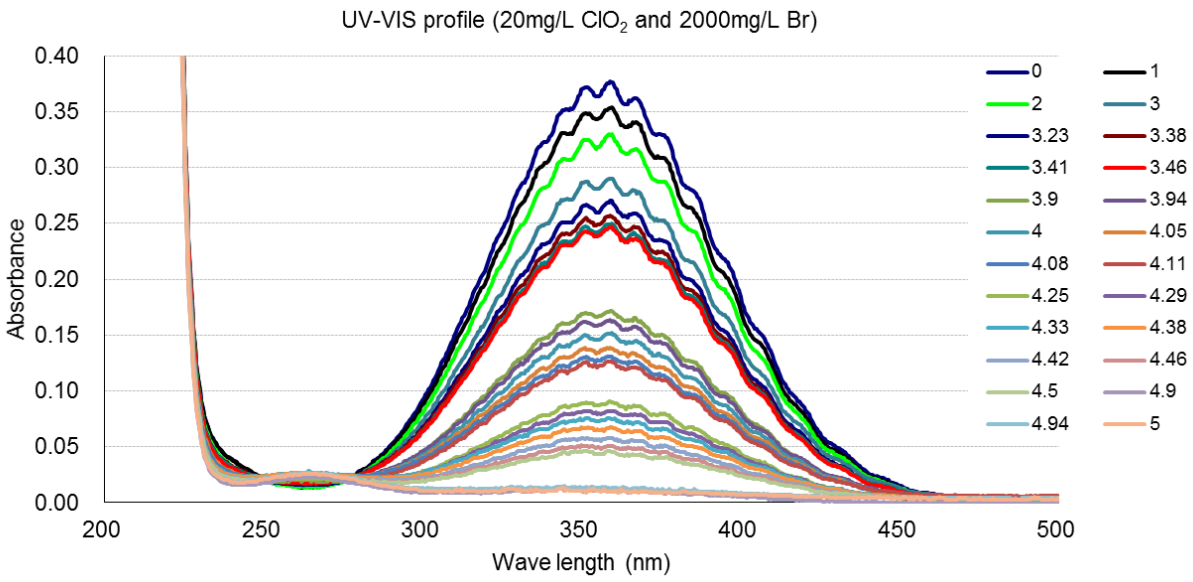

Figure A3. The UV-VIS spectrum over time. Experimental conditions correspond to 2000 mg/L Br disinfected with 20 mg/L ClO_2 at pH = 7.5 which was controlled by 10mM phosphate buffer solution.

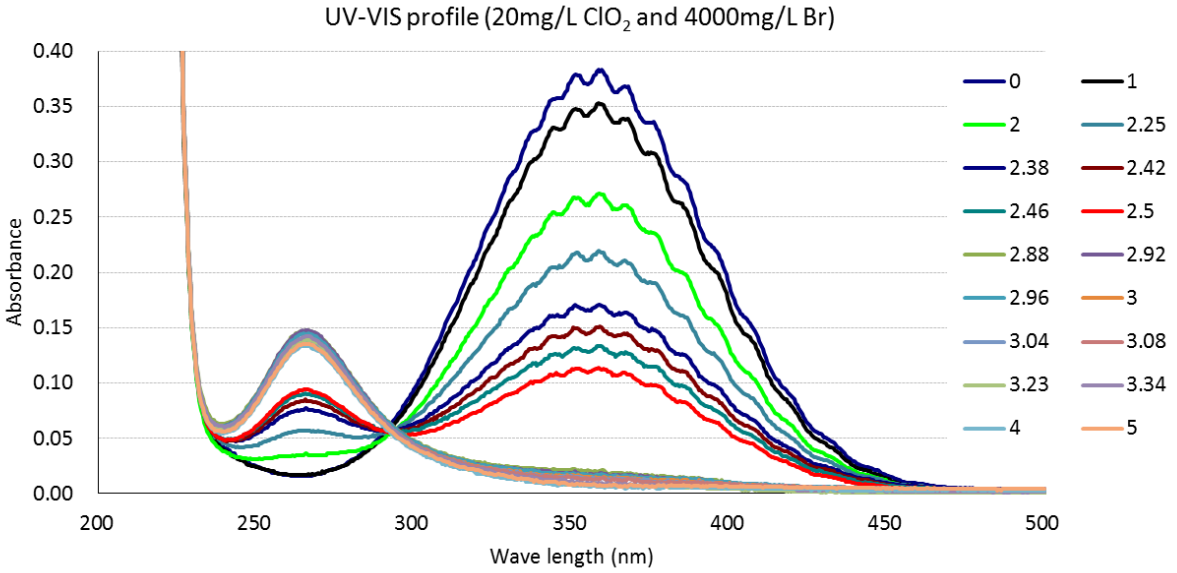

Figure A4. The UV-VIS spectrum over time. Experimental conditions correspond to 4000 mg/L Br disinfected with 20 mg/L ClO_2 at pH = 7.5 which was controlled by 10mM phosphate buffer solution.

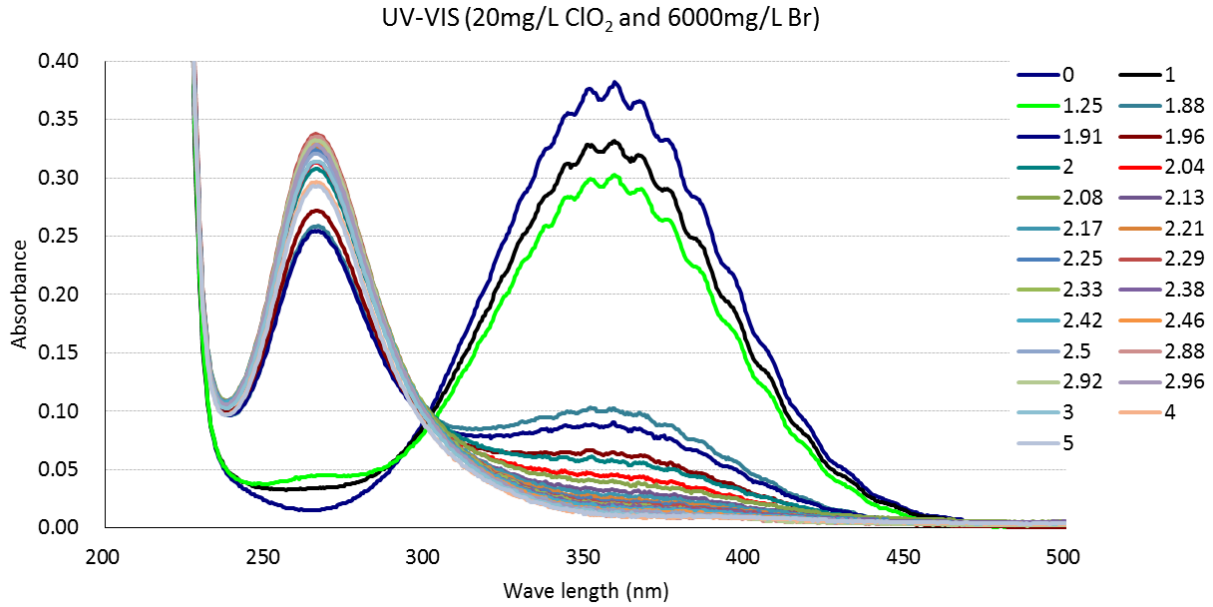

Figure A5. The UV-VIS spectrum over time. Experimental conditions correspond to 4000 mg/L Br disinfected with 20 mg/L ClO_2 at pH = 7.5 which was controlled by 10mM phosphate buffer solution.

Table A9. Raw data of UV absorbance (λ = 359 nm) and ClO_2 concentration over time. Experimental conditions correspond to 200 mg/L Br disinfected with 20 mg/L ClO_2 at pH = 7.5 which was controlled by 10mM phosphate buffer solution.

200 mg/L Br			
time (day)	ClO_2		
	Absorbance	(mg/L)	[mM]
0	0.340	18.7	0.276
1	0.324	17.8	0.263
2	0.306	16.8	0.249
3	0.293	16.1	0.238
4	0.285	15.6	0.232
5	0.270	14.8	0.220
6	0.258	14.2	0.210
7	0.261	14.3	0.212

Table A10. Raw data of UV absorbance of ClO_2 (λ = 359 nm, ε=1230 L M^{-1} cm^{-1}) and Br_3^- (λ = 266 nm, ε=35000 L M^{-1} cm^{-1}) over time. Each concentration was estimated by eq. (6), respectively. Experimental conditions correspond to 2000 mg/L Br disinfected with 20 mg/L ClO_2 at pH = 7.5 which was controlled by 10mM phosphate buffer solution.

2000 mg/L Br						
time (day)	ClO_2			Br_3^-		
	Absorbance	(mg/L)	[mM]	Absorbance	(mg/L)	[μM]
0	0.377	20.7	0.307	0.014	0.096	0.40
1	0.353	19.4	0.287	0.015	0.103	0.43
2	0.329	18.1	0.267	0.014	0.096	0.40
3	0.290	15.9	0.236	0.016	0.110	0.46
3.23	0.270	14.8	0.220	0.016	0.110	0.46
3.38	0.257	14.1	0.209	0.018	0.123	0.51
3.41	0.249	13.7	0.202	0.018	0.123	0.51
3.46	0.246	13.5	0.200	0.018	0.123	0.51
3.9	0.172	9.4	0.140	0.020	0.137	0.57
3.94	0.164	9.0	0.133	0.022	0.151	0.63
4	0.151	8.3	0.123	0.021	0.144	0.60
4.05	0.139	7.6	0.113	0.024	0.164	0.69
4.08	0.131	7.2	0.107	0.024	0.164	0.69
4.11	0.126	6.9	0.102	0.021	0.144	0.60
4.25	0.091	5.0	0.074	0.021	0.144	0.60
4.29	0.082	4.5	0.067	0.024	0.164	0.69
4.33	0.076	4.2	0.062	0.027	0.185	0.77
4.38	0.068	3.7	0.055	0.026	0.178	0.74
4.42	0.058	3.2	0.047	0.025	0.171	0.71
4.46	0.051	2.8	0.041	0.025	0.171	0.71
4.5	0.046	2.5	0.037	0.025	0.171	0.71
4.9	0.010	0.5	0.008	0.023	0.158	0.66
4.94	0.012	0.7	0.010	0.027	0.185	0.77
5	0.010	0.5	0.008	0.026	0.178	0.74

Table A11. Raw data of UV absorbance of ClO_2 (λ = 359 nm, ε=1230 L M^{-1} cm^{-1}) and Br_3^- (λ = 266 nm, ε=35000 L M^{-1} cm^{-1}) over time. Each concentration was estimated by eq. (6), respectively. Experimental conditions correspond to 4000 mg/L Br disinfected with 20 mg/L ClO_2 at pH = 7.5 which was controlled by 10mM phosphate buffer solution.

4000 mg/L Br						
time (day)	ClO_2			Br_3^-		
	Absorbance	(mg/L)	[mM]	Absorbance	(mg/L)	[μM]
0	0.382	21.0	0.311	0.016	0.110	0.46
1	0.352	19.3	0.286	0.017	0.116	0.49
2	0.271	14.9	0.220	0.036	0.247	1.03
2.25	0.219	12.0	0.178	0.057	0.390	1.63
2.38	0.171	9.4	0.139	0.077	0.527	2.20
2.42	0.151	8.3	0.123	0.084	0.575	2.40
2.46	0.133	7.3	0.108	0.090	0.616	2.57
2.5	0.113	6.2	0.092	0.094	0.644	2.69
2.88	0.020	1.1	0.016	0.148	1.014	4.23
2.92	0.019	1.0	0.015	0.148	1.014	4.23
2.96	0.017	0.9	0.014	0.144	0.986	4.11
3	0.014	0.8	0.011	0.140	0.959	4.00
3.04	0.013	0.7	0.011	0.138	0.945	3.94
3.08	0.013	0.7	0.011	0.141	0.966	4.03
3.23	0.008	0.4	0.007	0.140	0.959	4.00
3.34	0.009	0.5	0.007	0.142	0.972	4.06
4	0.006	0.3	0.005	0.133	0.911	3.80
5	0.008	0.4	0.007	0.135	0.925	3.86

Table A12. Raw data of UV absorbance of ClO_2 (λ = 359 nm, ε=1230 L M^{-1} cm^{-1}) and Br_3^- (λ = 266 nm, ε=35000 L M^{-1} cm^{-1}) over time. Each concentration was estimated by eq. (6), respectively. Experimental conditions correspond to 6000 mg/L Br disinfected with 20 mg/L ClO_2 at pH = 7.5 which was controlled by 10mM phosphate buffer solution.

6000 mg/L Br						
time (day)	ClO_2			Br_3^-		
	Absorbance	(mg/L)	[mM]	Absorbance	(mg/L)	[μM]
0	0.382	20.96	0.3106	0.015	0.10	0.43
1	0.332	18.22	0.2699	0.034	0.23	0.97
1.25	0.303	16.63	0.2463	0.045	0.31	1.29
1.88	0.102	5.60	0.0829	0.258	1.77	7.37
1.91	0.090	4.94	0.0732	0.254	1.74	7.26
1.96	0.065	3.57	0.0528	0.272	1.86	7.77
2	0.057	3.13	0.0463	0.308	2.11	8.80
2.04	0.045	2.47	0.0366	0.313	2.14	8.94
2.08	0.039	2.14	0.0317	0.323	2.21	9.23
2.13	0.032	1.76	0.0260	0.314	2.15	8.97
2.17	0.029	1.59	0.0236	0.325	2.23	9.29
2.21	0.025	1.37	0.0203	0.328	2.25	9.37
2.25	0.023	1.26	0.0187	0.323	2.21	9.23
2.29	0.022	1.21	0.0179	0.338	2.31	9.66
2.33	0.021	1.15	0.0171	0.335	2.29	9.57
2.38	0.020	1.10	0.0163	0.330	2.26	9.43
2.42	0.018	0.99	0.0146	0.333	2.28	9.51
2.46	0.016	0.88	0.0130	0.330	2.26	9.43
2.5	0.015	0.82	0.0122	0.321	2.20	9.17
2.88	0.010	0.55	0.0081	0.335	2.29	9.57
2.92	0.012	0.66	0.0098	0.332	2.27	9.49
2.96	0.014	0.77	0.0114	0.328	2.25	9.37
3	0.013	0.71	0.0106	0.314	2.15	8.97
4	0.014	0.77	0.0114	0.328	2.25	9.37
5	0.013	0.71	0.0106	0.314	2.15	8.97

APPENDIX B

SUPPLEMENTAL FIGURES AND TABLES OF MEMBRANE ANALYSIS

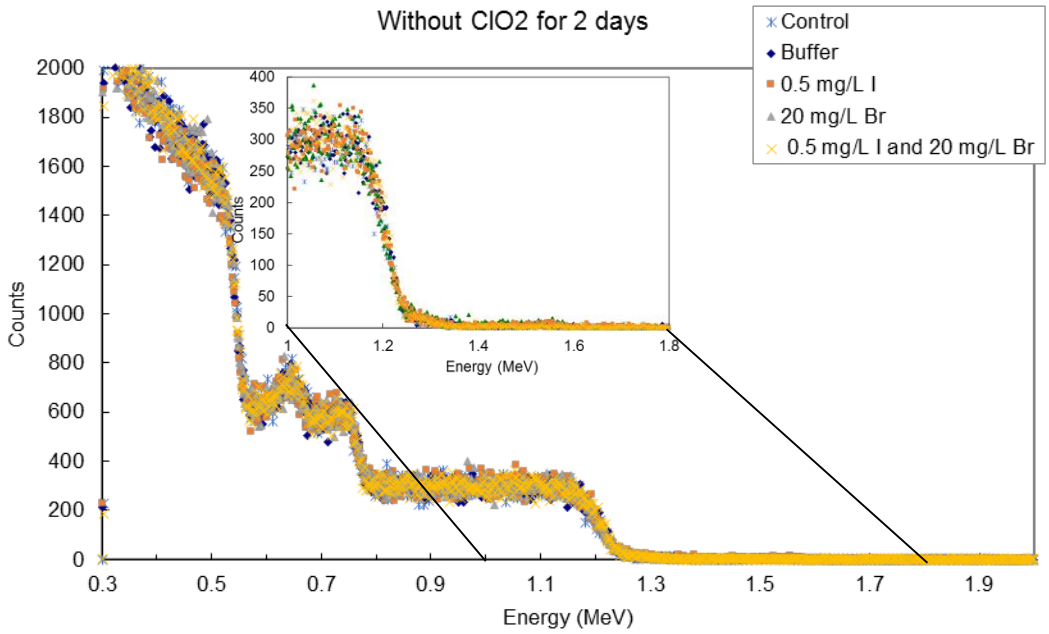

Figure B1. RBS characterization after SW30HR membrane exposure for 2 days. Experimental conditions for the Control correspond to 100 mL nanopure water. Experimental conditions for the Buffer correspond to 10mM phosphate buffer at pH 7.5. Experimental conditions for the 0.5 mg/L I correspond to 0.5 mg/L I and 10mM phosphate buffer at pH 7.5. Experimental conditions for the 20 mg/L Br correspond to 20 mg/L Br and 10mM phosphate buffer at pH 7.5. Experimental conditions for the 0.5 mg/L I and 20 mg/L Br correspond to 0.5 mg/L I and 20 mg/L Br and 10mM phosphate buffer at pH 7.5.

Table B1. Atomic concentration (atoms element/atoms PA) data from membrane exposure for 2 days. Experimental conditions for the Control correspond to 100 mL nanopure water. Experimental conditions for the Buffer correspond to 10mM phosphate buffer at pH 7.5. Experimental conditions for the 0.5 mg/L I correspond to 0.5 mg/L I and 10mM phosphate buffer at pH 7.5. Experimental conditions for the 20 mg/L Br correspond to 20 mg/L Br and 10mM phosphate buffer at pH 7.5. Experimental conditions for the 0.5 mg/L I and 20 mg/L Br correspond to 0.5 mg/L I and 20 mg/L Br and 10mM phosphate buffer at pH 7.5.

atomic (atoms element/atoms PA)									
Description	Layer thickness [atoms/cm2]	%C	%O	%N	%H	%K	%Cl	%I	%Br
Contorol	870	41.0%	8.0%	6.5%	44.4%	0.020%	0.070%	0.0000%	0.0000%
Buffer	1000	41.0%	7.5%	6.5%	44.9%	0.020%	0.090%	0.0000%	0.0000%
ClO2, I−	880	41.0%	7.8%	6.5%	44.6%	0.020%	0.070%	0.0000%	0.0000%
ClO2, Br−	950	41.0%	7.5%	6.2%	45.2%	0.040%	0.060%	0.0000%	0.0000%
ClO2, I−, Br−	870	41.0%	7.3%	6.9%	44.7%	0.000%	0.090%	0.0000%	0.0000%

Table B2. Concentration data by weight (g element/g PA) from membrane exposure for 2 days. Experimental conditions for the Control correspond to 100 mL nanopure water. Experimental conditions for the Buffer correspond to 10mM phosphate buffer at pH 7.5. Experimental conditions for the 0.5 mg/L I correspond to 0.5 mg/L I and 10mM phosphate buffer at pH 7.5. Experimental conditions for the 20 mg/L Br correspond to 20 mg/L Br and 10mM phosphate buffer at pH 7.5. Experimental conditions for the 0.5 mg/L I and 20 mg/L Br correspond to 0.5 mg/L I and 20 mg/L Br and 10mM phosphate buffer at pH 7.5.

weight (g element/g PA) without the ion							
Description	denominator=∑（εi × Mi）	%C	%O	%N	%H	%K	%Cl
Contorol	7.59E+00	64.85%	16.87%	11.99%	5.85%	0.10%	0.33%
Buffer	7.52E+00	65.44%	15.96%	12.10%	5.97%	0.10%	0.42%
ClO2, I−	7.56E+00	65.11%	16.51%	12.04%	5.90%	0.10%	0.33%
ClO2, Br−	7.48E+00	65.80%	16.05%	11.61%	6.05%	0.21%	0.28%
ClO2, I−, Br−	7.53E+00	65.31%	15.51%	12.82%	5.94%	0.00%	0.42%

Table B3. Concentration data by weight (g element/g PA) and by volume (g element/L PA) from membrane exposure for 2 days. Experimental conditions for the Control correspond to 100 mL nanopure water. Experimental conditions for the Buffer correspond to 10mM phosphate buffer at pH 7.5. Experimental conditions for the 0.5 mg/L I correspond to 0.5 mg/L I and 10mM phosphate buffer at pH 7.5. Experimental conditions for the 20 mg/L Br correspond to 20 mg/L Br and 10mM phosphate buffer at pH 7.5. Experimental conditions for the 0.5 mg/L I and 20 mg/L Br correspond to 0.5 mg/L I and 20 mg/L Br and 10mM phosphate buffer at pH 7.5.

molar concentration								
Description	[mol I /g PA]	[mol Br /g PA]	[mol K /g PA]	[mol Cl /g PA]	mol I/L	mol Br/L	mol K/L	mol Cl/L
Contorol	0.00E+00	0.00E+00	1.62E−05	5.66E−05	0.000	0.00	0.02	0.07
Buffer	0.00E+00	0.00E+00	1.62E−05	7.29E−05	0.000	0.00	0.02	0.09
ClO2, I−	0.00E+00	0.00E+00	1.62E−05	5.66E−05	0.000	0.00	0.02	0.07
ClO2, Br−	0.00E+00	0.00E+00	3.24E−05	4.87E−05	0.000	0.00	0.04	0.06
ClO2, I−, Br−	0.00E+00	0.00E+00	0.00E+00	7.30E−05	0.000	0.00	0.00	0.09

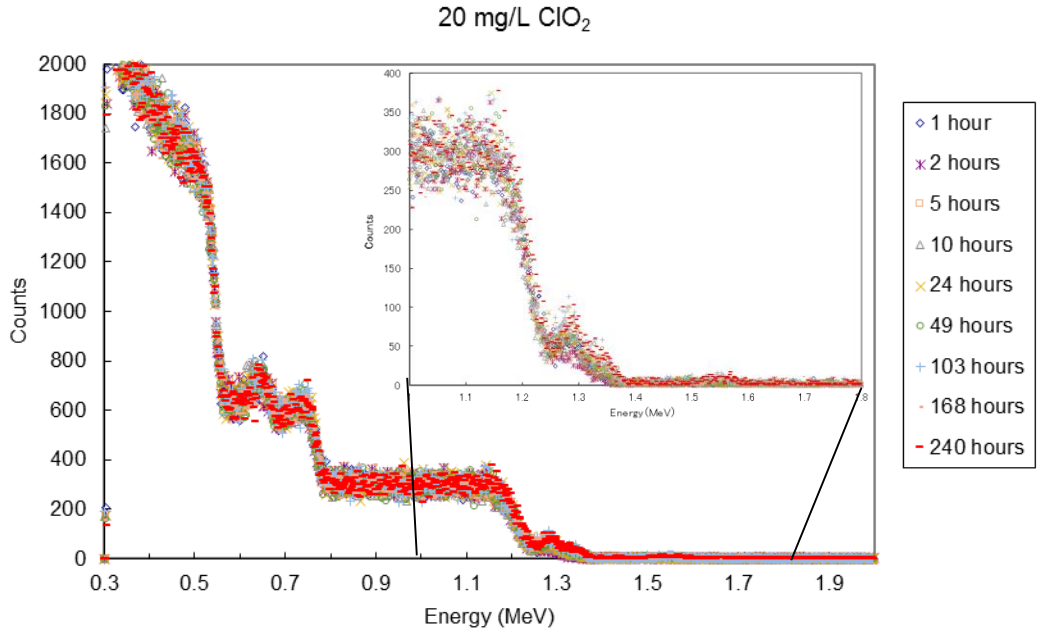

Figure B2. RBS characterization after SW30HR membrane exposure to 20 mg/L ClO_2 as disinfection. Data points obtained using SIMNRA based on RBS analysis data.

Table B4. Atomic concentration (atoms element/atoms PA) data from membrane exposure to 20 mg/L ClO_2.

atomic (atoms element/atoms PA)									
hour	Layer thickness [atoms/cm2]	%C	%O	%N	%H	%K	%Cl	%I	%Br
1	850	42.0%	8.3%	6.6%	42.7%	0.040%	0.350%	0.0000%	0.0000%
2	890	41.0%	7.7%	6.1%	44.9%	0.040%	0.230%	0.0000%	0.0000%
5	800	40.0%	8.4%	6.9%	44.4%	0.070%	0.280%	0.0000%	0.0000%
10	900	42.0%	8.1%	6.4%	43.0%	0.030%	0.495%	0.0000%	0.0000%
24	850	43.0%	8.7%	6.5%	41.3%	0.070%	0.460%	0.0000%	0.0000%
49	850	41.0%	9.1%	6.6%	42.8%	0.100%	0.380%	0.0000%	0.0000%
103	850	42.0%	8.9%	6.4%	42.0%	0.120%	0.620%	0.0000%	0.0000%
168	810	44.0%	8.8%	6.4%	40.1%	0.130%	0.590%	0.0000%	0.0000%
240	820	42.0%	8.2%	6.8%	42.3%	0.190%	0.550%	0.0000%	0.0000%

Table B5. Concentration data by weight (g element/g PA) from membrane exposure to 20 mg/L ClO_2.

weight (g element/g PA) without the ion							
hour	denominator=Σ（εi × Mi）	%C	%O	%N	%H	%K	%Cl
1	7.86E+00	64.13%	16.90%	11.76%	5.43%	0.20%	1.58%
2	7.55E+00	65.14%	16.31%	11.31%	5.95%	0.21%	1.08%
5	7.68E+00	62.50%	17.50%	12.58%	5.77%	0.36%	1.29%
10	7.85E+00	64.21%	16.51%	11.42%	5.48%	0.15%	2.24%
24	8.07E+00	63.98%	17.26%	11.28%	5.12%	0.34%	2.02%
49	7.90E+00	62.26%	18.43%	11.69%	5.42%	0.49%	1.71%
103	8.05E+00	62.63%	17.70%	11.14%	5.21%	0.58%	2.74%
168	8.25E+00	64.04%	17.08%	10.87%	4.86%	0.62%	2.54%
240	8.00E+00	63.03%	16.41%	11.91%	5.29%	0.93%	2.44%

Table B6. Concentration data by weight (g element/g PA) and by volume (g element/L PA) from membrane exposure to 20 mg/L ClO_2.

molar concentration								
hour	[mol I /g PA]	[mol Br /g PA]	[mol K /g PA]	[mol Cl /g PA]	mol I/L	mol Br/L	mol K/L	mol Cl/L
1	0.00E+00	0.00E+00	3.14E-05	2.75E-04	0.000	0.00	0.04	0.34
2	0.00E+00	0.00E+00	3.19E-05	1.83E-04	0.000	0.00	0.04	0.23
5	0.00E+00	0.00E+00	5.50E-05	2.20E-04	0.000	0.00	0.07	0.27
10	0.00E+00	0.00E+00	2.33E-05	3.85E-04	0.000	0.00	0.03	0.48
24	0.00E+00	0.00E+00	5.42E-05	3.56E-04	0.000	0.00	0.07	0.44
49	0.00E+00	0.00E+00	7.75E-05	2.94E-04	0.000	0.00	0.10	0.36
103	0.00E+00	0.00E+00	9.12E-05	4.71E-04	0.000	0.00	0.11	0.58
168	0.00E+00	0.00E+00	9.90E-05	4.49E-04	0.000	0.00	0.12	0.56
240	0.00E+00	0.00E+00	1.45E-04	4.19E-04	0.000	0.00	0.18	0.52

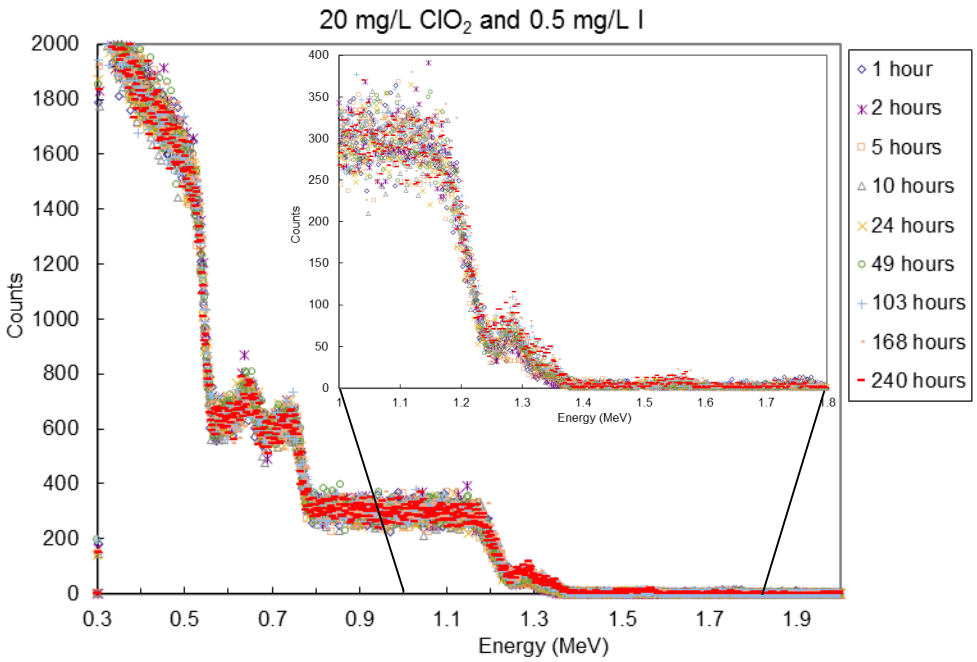

Figure B3. RBS characterization after SW30HR membrane exposure to 0.5 mg/L I disinfected with 20 mg/L ClO_2. Data points obtained using SIMNRA based on RBS analysis data.

Table B7. Atomic concentration (atoms element/atoms PA) data from membrane exposure to 0.5 mg/L I disinfected with 20 mg/L ClO_2.

atomic (atoms element/atoms PA)									
hour	Layer thickness [atoms/cm2]	%C	%O	%N	%H	%K	%Cl	%I	%Br
1	840	42.0%	8.3%	6.5%	42.7%	0.035%	0.440%	0.0075%	0.0000%
2	830	45.0%	8.8%	6.5%	39.3%	0.040%	0.350%	0.0040%	0.0000%
5	800	40.0%	8.9%	6.0%	44.8%	0.040%	0.300%	0.0050%	0.0000%
10	820	40.0%	8.6%	6.5%	44.4%	0.050%	0.470%	0.0040%	0.0000%
24	860	44.0%	8.7%	6.5%	40.3%	0.060%	0.460%	0.0040%	0.0000%
49	840	43.0%	9.1%	6.8%	40.6%	0.080%	0.450%	0.0030%	0.0000%
103	830	44.0%	9.6%	6.5%	39.2%	0.130%	0.610%	0.0040%	0.0000%
168	800	45.0%	8.9%	6.3%	39.1%	0.160%	0.570%	0.0040%	0.0000%
240	820	42.0%	8.9%	6.8%	41.6%	0.160%	0.580%	0.0040%	0.0000%

Table B8. Concentration data by weight (g element/g PA) from membrane exposure to 0.5 mg/L I disinfected with 20 mg/L ClO_2.

weight (g element/g PA) without the ion							
hour	denominator=Σ（εi × Mi）	%C	%O	%N	%H	%K	%Cl
1	7.88E+00	64.00%	16.86%	11.56%	5.42%	0.17%	1.98%
2	8.25E+00	65.45%	17.06%	11.03%	4.76%	0.19%	1.51%
5	7.63E+00	62.88%	18.65%	11.00%	5.86%	0.20%	1.40%
10	7.72E+00	62.21%	17.83%	11.79%	5.75%	0.25%	2.16%
24	8.17E+00	64.61%	17.03%	11.14%	4.93%	0.29%	2.00%
49	8.16E+00	63.20%	17.83%	11.66%	4.97%	0.38%	1.96%
103	8.38E+00	62.97%	18.32%	10.85%	4.67%	0.61%	2.58%
168	8.36E+00	64.58%	17.03%	10.55%	4.67%	0.75%	2.42%
240	8.10E+00	62.22%	17.58%	11.75%	5.13%	0.77%	2.54%

Table B9. Concentration data by weight (g element/g PA) and by volume (g element/L PA) from membrane exposure to 0.5 mg/L I disinfected with 20 mg/L ClO_2.

molar concentration								
hour	[mol I /g PA]	[mol Br /g PA]	[mol K /g PA]	[mol Cl /g PA]	mol I/L	mol Br/L	mol K/L	mol Cl/L
1	5.85E-06	0.00E+00	2.73E-05	3.43E-04	0.007	0.00	0.03	0.43
2	3.13E-06	0.00E+00	3.13E-05	2.74E-04	0.004	0.00	0.04	0.34
5	3.94E-06	0.00E+00	3.15E-05	2.36E-04	0.005	0.00	0.04	0.29
10	3.10E-06	0.00E+00	3.88E-05	3.65E-04	0.004	0.00	0.05	0.45
24	3.10E-06	0.00E+00	4.65E-05	3.56E-04	0.004	0.00	0.06	0.44
49	2.31E-06	0.00E+00	6.17E-05	3.47E-04	0.003	0.00	0.08	0.43
103	3.03E-06	0.00E+00	9.84E-05	4.62E-04	0.004	0.00	0.12	0.57
168	3.04E-06	0.00E+00	1.22E-04	4.33E-04	0.004	0.00	0.15	0.54
240	3.03E-06	0.00E+00	1.21E-04	4.40E-04	0.004	0.00	0.15	0.55

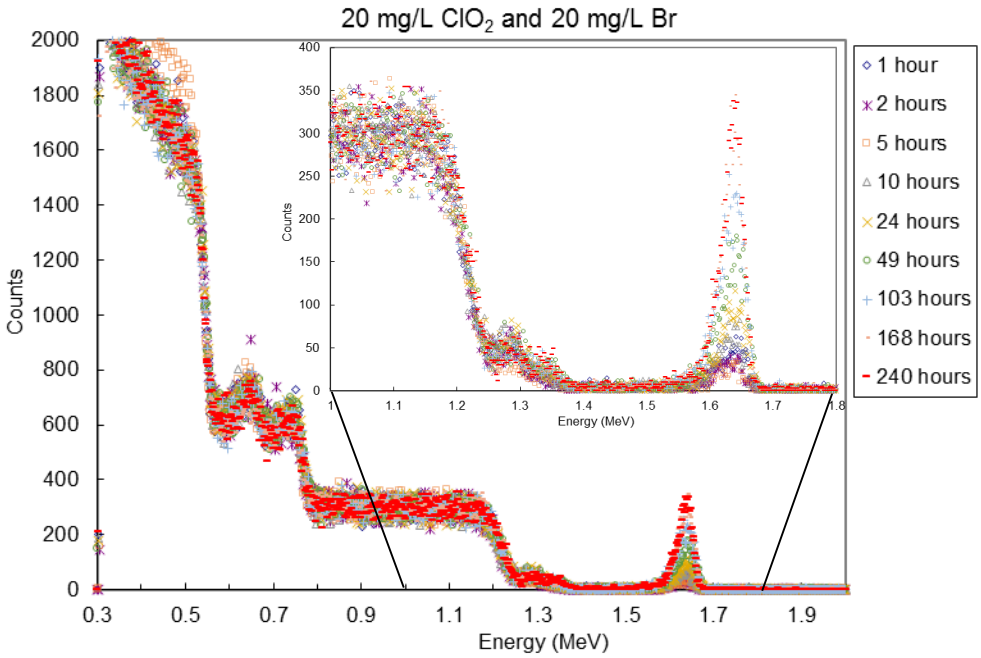

Figure B4. RBS characterization after SW30HR membrane exposure to 20 mg/L Br disinfected with 20 mg/L ClO_2. Data points obtained using SIMNRA based on RBS analysis data.

Table B10. Atomic concentration (atoms element/atoms PA) data from membrane exposure to 20 mg/L Br disinfected with 20 mg/L ClO_2.

atomic (atoms element/atoms PA)									
hour	Layer thickness [atoms/cm2]	%C	%O	%N	%H	%K	%Cl	%I	%Br
1	840	42.0%	8.5%	6.8%	42.3%	0.040%	0.310%	0.0000%	0.0730%
2	810	42.0%	8.2%	6.9%	42.5%	0.020%	0.320%	0.0000%	0.0440%
5	810	41.0%	7.5%	6.8%	44.4%	0.045%	0.170%	0.0000%	0.0410%
10	860	41.0%	8.6%	6.0%	43.8%	0.040%	0.410%	0.0000%	0.1110%
24	800	42.0%	8.9%	6.9%	41.6%	0.060%	0.410%	0.0000%	0.1500%
49	800	42.0%	9.3%	6.7%	41.3%	0.110%	0.370%	0.0000%	0.2500%
103	810	40.0%	8.6%	6.4%	44.2%	0.090%	0.340%	0.0000%	0.3300%
168	800	40.0%	7.2%	6.0%	45.9%	0.100%	0.340%	0.0000%	0.4900%
240	760	42.0%	8.4%	6.8%	41.8%	0.160%	0.300%	0.0000%	0.5150%

Table B11. Concentration data by weight (g element/g PA) from membrane exposure to 20 mg/L Br disinfected with 20 mg/L ClO_2.

weight (g element/g PA) without the ion							
hour	denominator=Σ（εi × Mi）	%C	%O	%N	%H	%K	%Cl
1	7.90E+00	63.79%	17.21%	12.05%	5.35%	0.20%	1.39%
2	7.86E+00	64.08%	16.68%	12.28%	5.41%	0.10%	1.44%
5	7.59E+00	64.78%	15.80%	12.54%	5.85%	0.23%	0.79%
10	7.74E+00	63.60%	17.79%	10.86%	5.67%	0.20%	1.88%
24	8.01E+00	62.88%	17.77%	12.05%	5.19%	0.29%	1.82%
49	8.05E+00	62.58%	18.48%	11.65%	5.12%	0.53%	1.63%
103	7.67E+00	62.58%	17.94%	11.68%	5.77%	0.46%	1.57%
168	7.41E+00	64.77%	15.55%	11.34%	6.19%	0.53%	1.63%
240	7.92E+00	63.61%	16.96%	12.02%	5.28%	0.79%	1.34%

Table B12. Concentration data by weight (g element/g PA) and by volume (g element/L PA) from membrane exposure to 20 mg/L Br disinfected with 20 mg/L ClO_2.

molar concentration								
hour	[mol I /g PA]	[mol Br /g PA]	[mol K /g PA]	[mol Cl /g PA]	mol I/L	mol Br/L	mol K/L	mol Cl/L
1	0.00E+00	5.74E-05	3.14E-05	2.44E-04	0.000	0.07	0.04	0.30
2	0.00E+00	3.47E-05	1.58E-05	2.52E-04	0.000	0.04	0.02	0.31
5	0.00E+00	3.28E-05	3.60E-05	1.36E-04	0.000	0.04	0.04	0.17
10	0.00E+00	8.67E-05	3.12E-05	3.20E-04	0.000	0.11	0.04	0.40
24	0.00E+00	1.16E-04	4.66E-05	3.18E-04	0.000	0.14	0.06	0.39
49	0.00E+00	1.93E-04	8.50E-05	2.86E-04	0.000	0.24	0.11	0.35
103	0.00E+00	2.58E-04	7.03E-05	2.65E-04	0.000	0.32	0.09	0.33
168	0.00E+00	3.86E-04	7.88E-05	2.68E-04	0.000	0.48	0.10	0.33
240	0.00E+00	4.00E-04	1.24E-04	2.33E-04	0.000	0.50	0.15	0.29

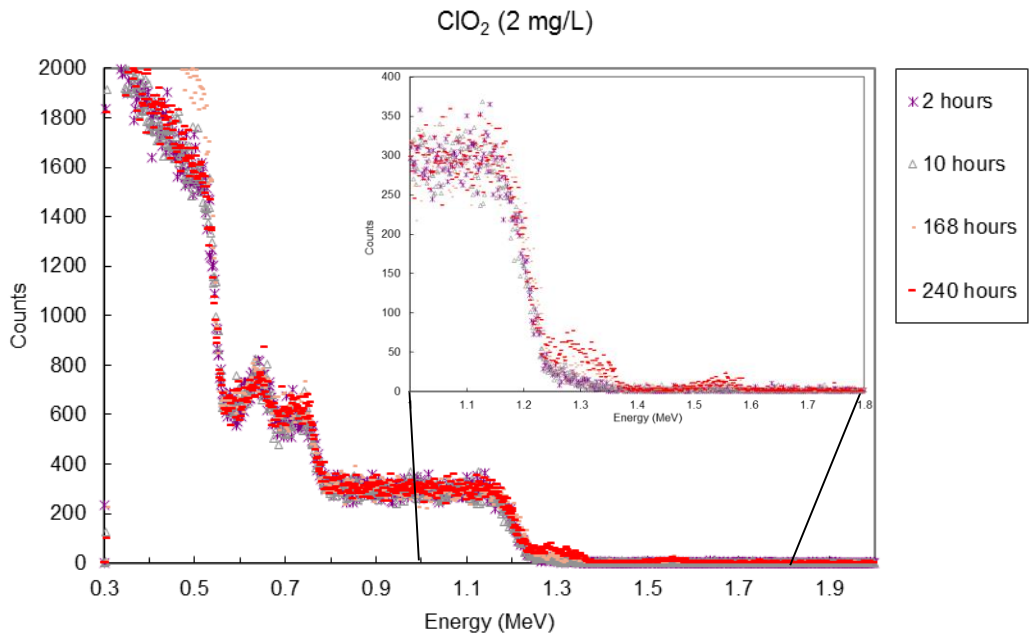

Figure B5. RBS characterization after SW30HR membrane exposure to 2 mg/L ClO_2 as disinfection. Data points obtained using SIMNRA based on RBS analysis data.

Table B13. Atomic concentration (atoms element/atoms PA) data from membrane exposure to 2 mg/L ClO_2.

atomic (atoms element/atoms PA)									
hour	Layer thickness [atoms/cm2]	%C	%O	%N	%H	%K	%Cl	%I	%Br
2	900	42.0%	7.2%	6.9%	43.8%	0.040%	0.090%	0.0000%	0.0000%
10	880	42.0%	7.0%	6.9%	44.0%	0.030%	0.110%	0.0000%	0.0000%
168	850	47.0%	7.5%	6.9%	38.4%	0.080%	0.110%	0.0000%	0.0000%
240	840	42.0%	8.6%	6.1%	42.8%	0.160%	0.390%	0.0000%	0.0000%

Table B14. Concentration data by weight (g element/g PA) from membrane exposure to 2 mg/L ClO_2.

weight (g element/g PA) without the ion							
hour	denominator=Σ（εi × Mi）	%C	%O	%N	%H	%K	%Cl
2	7.64E+00	65.94%	15.07%	12.64%	5.73%	0.20%	0.42%
10	7.62E+00	66.17%	14.71%	12.68%	5.77%	0.15%	0.51%
168	8.26E+00	68.28%	14.53%	11.69%	4.65%	0.38%	0.47%
240	7.90E+00	63.81%	17.42%	10.81%	5.41%	0.79%	1.75%

Table B15. Concentration data by weight (g element/g PA) and by volume (g element/L PA) from membrane exposure to 2 mg/L ClO_2.

molar concentration								
hour	[mol I /g PA]	[mol Br /g PA]	[mol K /g PA]	[mol Cl /g PA]	mol I/L	mol Br/L	mol K/L	mol Cl/L
2	0.00E+00	0.00E+00	3.23E-05	7.27E-05	0.000	0.00	0.04	0.09
10	0.00E+00	0.00E+00	2.43E-05	8.89E-05	0.000	0.00	0.03	0.11
168	0.00E+00	0.00E+00	6.39E-05	8.79E-05	0.000	0.00	0.08	0.11
240	0.00E+00	0.00E+00	1.24E-04	3.01E-04	0.000	0.00	0.15	0.37

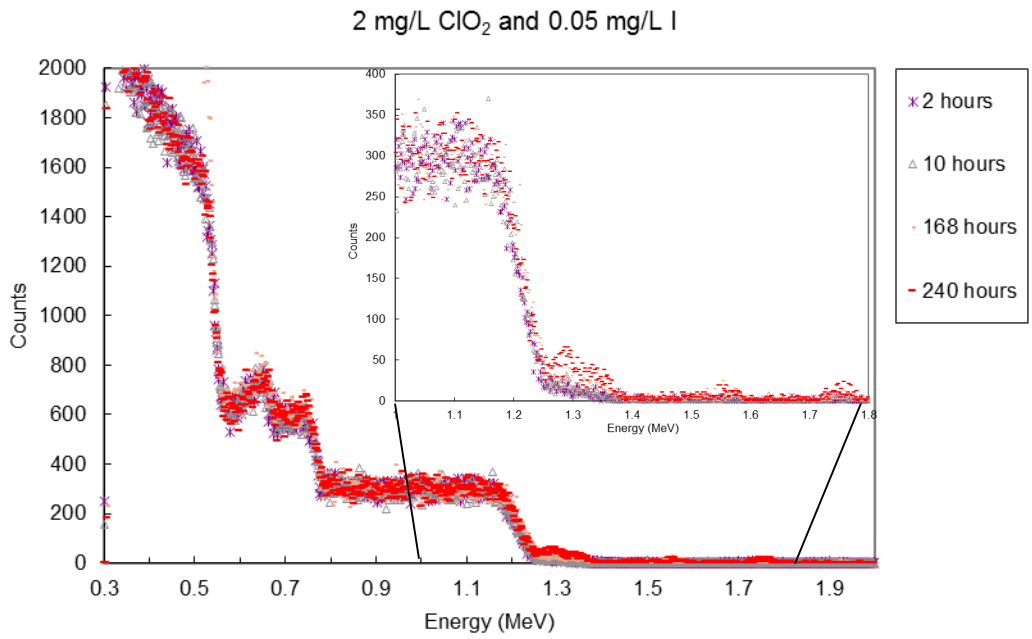

Figure B6. RBS characterization after SW30HR membrane exposure to 0.05 mg/L I disinfected with 2 mg/L ClO_2. Data points obtained using SIMNRA based on RBS analysis data.

Table B16. Atomic concentration (atoms element/atoms PA) data from membrane exposure to 0.05 mg/L I disinfected with 2 mg/L ClO_2.

atomic (atoms element/atoms PA)									
hour	Layer thickness [atoms/cm2]	%C	%O	%N	%H	%K	%Cl	%I	%Br
2	800	42.0%	6.9%	6.5%	44.5%	0.040%	0.090%	0.0020%	0.0000%
10	820	42.0%	7.9%	6.5%	43.4%	0.020%	0.140%	0.0035%	0.0000%
168	770	49.0%	7.3%	6.9%	36.6%	0.070%	0.170%	0.0040%	0.0000%
240	800	42.0%	8.8%	6.7%	42.0%	0.120%	0.330%	0.0120%	0.0000%

Table B17. Concentration data by weight (g element/g PA) from membrane exposure to 0.05 mg/L I disinfected with 2 mg/L ClO_2.

weight (g element/g PA) without the ion							
hour	denominator=Σ（εi × Mi）	%C	%O	%N	%H	%K	%Cl
2	7.55E+00	66.79%	14.63%	12.06%	5.89%	0.21%	0.42%
10	7.71E+00	65.40%	16.40%	11.81%	5.64%	0.10%	0.64%
168	8.47E+00	69.44%	13.79%	11.41%	4.32%	0.32%	0.71%
240	7.97E+00	63.23%	17.67%	11.77%	5.27%	0.59%	1.47%

Table B18. Concentration data by weight (g element/g PA) and by volume (g element/L PA) from membrane exposure to 0.5 mg/L I disinfected with 20 mg/L ClO_2.

molar concentration								
hour	[mol I /g PA]	[mol Br /g PA]	[mol K /g PA]	[mol Cl /g PA]	mol I/L	mol Br/L	mol K/L	mol Cl/L
2	1.62E-06	0.00E+00	3.24E-05	7.30E-05	0.002	0.00	0.04	0.09
10	2.81E-06	0.00E+00	1.61E-05	1.12E-04	0.003	0.00	0.02	0.14
168	3.18E-06	0.00E+00	5.57E-05	1.35E-04	0.004	0.00	0.07	0.17
240	9.33E-06	0.00E+00	9.33E-05	2.56E-04	0.012	0.00	0.12	0.32

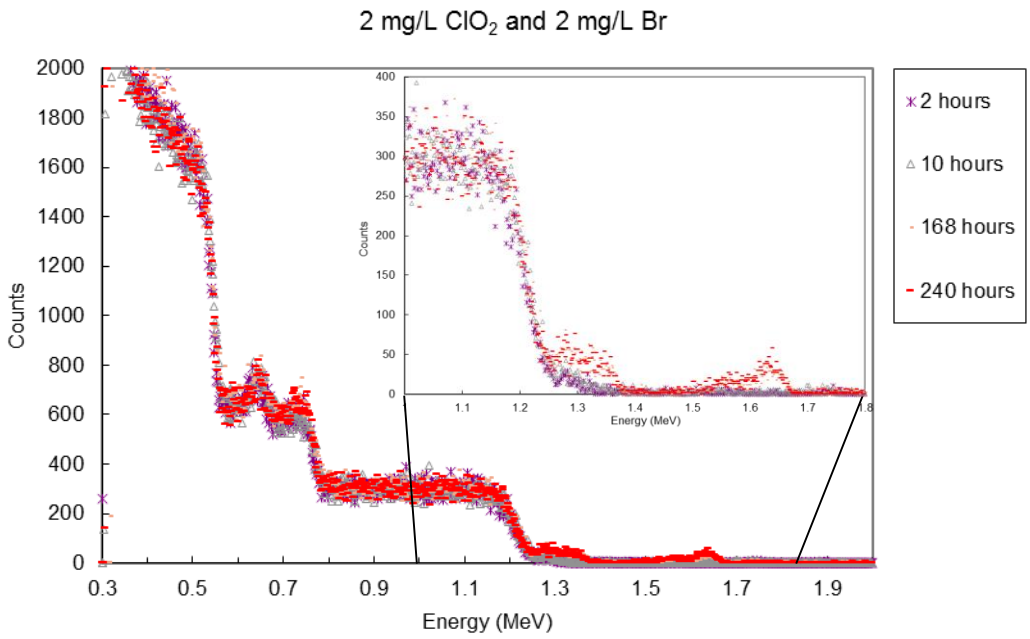

Figure B7. RBS characterization after SW30HR membrane exposure to 2 mg/L Br disinfected with 2 mg/L ClO_2. Data points obtained using SIMNRA based on RBS analysis data.

Table B19. Atomic concentration (atoms element/atoms PA) data from membrane exposure to 2 mg/L Br disinfected with 2 mg/L ClO_2.

atomic (atoms element/atoms PA)									
hour	Layer thickness [atoms/cm2]	%C	%O	%N	%H	%K	%Cl	%I	%Br
2	800	42.0%	7.2%	6.0%	44.6%	0.040%	0.140%	0.0000%	0.0060%
10	820	45.0%	7.6%	6.9%	40.3%	0.015%	0.180%	0.0000%	0.0087%
168	810	41.0%	9.0%	6.9%	42.6%	0.150%	0.310%	0.0000%	0.0450%
240	810	42.0%	8.8%	6.8%	41.8%	0.170%	0.370%	0.0000%	0.0680%

Table B20. Concentration data by weight (g element/g PA) from membrane exposure to 2 mg/L Br disinfected with 2 mg/L ClO_2.

weight (g element/g PA) without the ion							
hour	denominator=Σ（εi × Mi）	%C	%O	%N	%H	%K	%Cl
2	7.54E+00	66.81%	15.27%	11.14%	5.91%	0.21%	0.66%
10	8.05E+00	67.04%	15.10%	11.99%	5.00%	0.07%	0.79%
168	7.92E+00	62.12%	18.18%	12.20%	5.38%	0.74%	1.39%
240	8.02E+00	62.88%	17.57%	11.88%	5.21%	0.83%	1.64%

Table B21. Concentration data by weight (g element/g PA) and by volume (g element/L PA) from membrane exposure to 2 mg/L Br disinfected with 2 mg/L ClO_2.

molar concentration								
hour	[mol I /g PA]	[mol Br /g PA]	[mol K /g PA]	[mol Cl /g PA]	mol I/L	mol Br/L	mol K/L	mol Cl/L
2	0.00E+00	4.84E-06	3.23E-05	1.13E-04	0.000	0.01	0.04	0.14
10	0.00E+00	6.96E-06	1.20E-05	1.44E-04	0.000	0.01	0.01	0.18
168	0.00E+00	3.49E-05	1.16E-04	2.40E-04	0.000	0.04	0.14	0.30
240	0.00E+00	5.24E-05	1.31E-04	2.85E-04	0.000	0.06	0.16	0.35

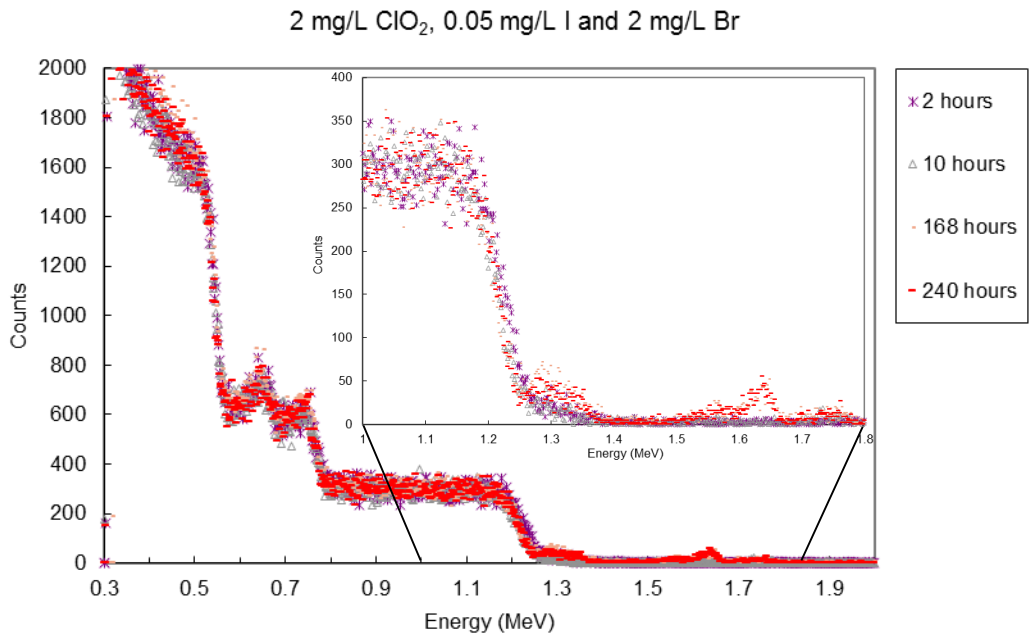

Figure B8. RBS characterization after SW30HR membrane exposure to 2 mg/L Br and 0.05 mg/L I disinfected with 2 mg/L ClO_2. Data points obtained using SIMNRA based on RBS analysis data.

Table B22. Atomic concentration (atoms element/atoms PA) data from membrane exposure to 2 mg/L Br and 0.05 mg/L I disinfected with 2 mg/L ClO_2.

atomic (atoms element/atoms PA)									
hour	Layer thickness [atoms/cm2]	%C	%O	%N	%H	%K	%Cl	%I	%Br
2	800	42.0%	7.6%	6.0%	44.2%	0.030%	0.150%	0.0030%	0.0030%
10	820	42.0%	8.1%	6.8%	42.8%	0.030%	0.230%	0.0095%	0.0080%
168	820	40.0%	9.1%	6.9%	43.5%	0.110%	0.370%	0.0090%	0.0580%
240	810	42.0%	8.6%	6.8%	42.1%	0.150%	0.300%	0.0091%	0.0610%

Table B23. Concentration data by weight (g element/g PA) from membrane exposure to 2 mg/L Br and 0.05 mg/L I disinfected with 2 mg/L ClO_2.

weight (g element/g PA) without the ion							
hour	denominator=Σ（εi × Mi）	%C	%O	%N	%H	%K	%Cl
2	7.60E+00	66.29%	15.99%	11.05%	5.82%	0.15%	0.70%
10	7.81E+00	64.54%	16.59%	12.19%	5.48%	0.15%	1.05%
168	7.83E+00	61.30%	18.59%	12.34%	5.55%	0.55%	1.68%
240	7.95E+00	63.36%	17.30%	11.97%	5.29%	0.74%	1.34%

Table B24. Concentration data by weight (g element/g PA) and by volume (g element/L PA) from membrane exposure to 2 mg/L Br and 0.05 mg/L I disinfected with 2 mg/L ClO_2.

molar concentration								
hour	[mol I /g PA]	[mol Br /g PA]	[mol K /g PA]	[mol Cl /g PA]	mol I/L	mol Br/L	mol K/L	mol Cl/L
2	2.41E-06	2.41E-06	2.41E-05	1.21E-04	0.003	0.00	0.03	0.15
10	7.55E-06	6.35E-06	2.38E-05	1.83E-04	0.009	0.01	0.03	0.23
168	6.96E-06	4.49E-05	8.51E-05	2.86E-04	0.009	0.06	0.11	0.36
240	7.07E-06	4.74E-05	1.17E-04	2.33E-04	0.009	0.06	0.14	0.29

APPENDIX C

SUPPLEMENTAL FIGURES AND TABLES OF PERMEATION EXPERIMENTS

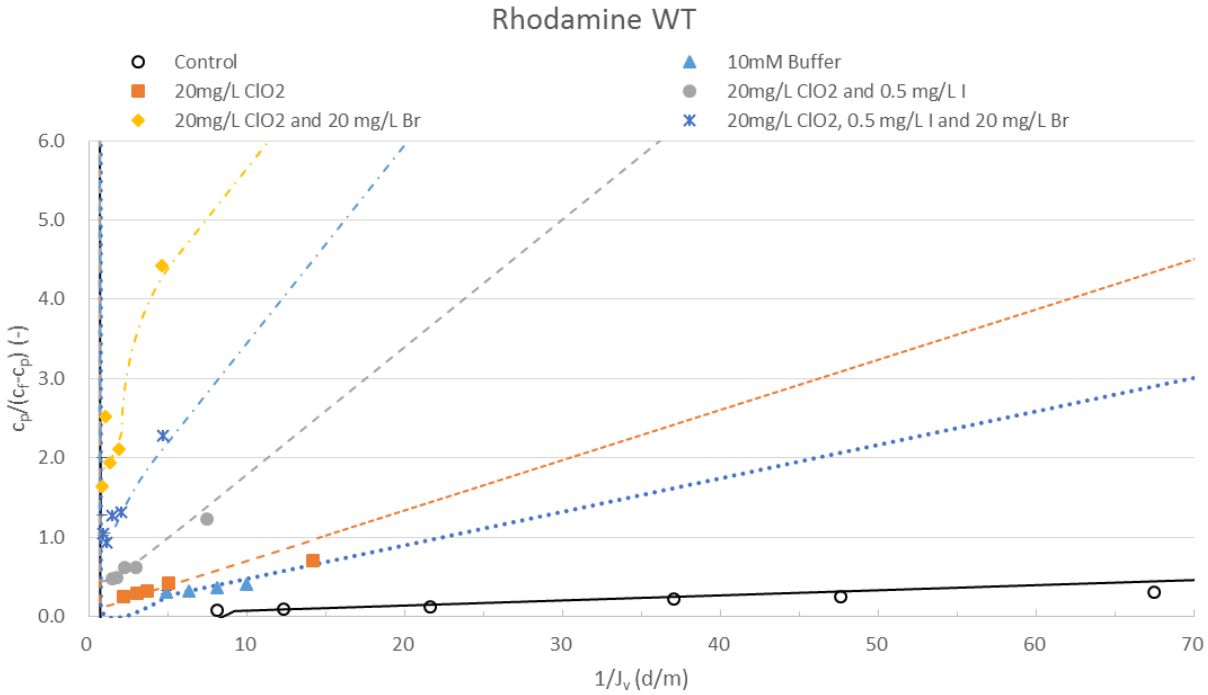

Figure C1. Experimental (symbols) and fitted (lines) solute permeation for Rhodamine WT rejection experiments. Opened circle represents the pure RO membrane soaking with nanopure water at least 24 hours, closed triangle represents the RO membrane exposure to 10 mM phosphate buffer solution at pH 7.5 for 10 days, closed square, closed circle closed diamond and asterisk represent RO membranes exposure to no compounds, 0.5 mg/L I, 20 mg/L Br, 0.5 mg/L I and 20 mg/L Br, disinfected with 20 mg/L ClO2 with 10 mM phosphate buffer solution at pH 7.5 for 10 days, respectively.